International Journal of Experimental Research and Review (IJERR)
 ISSN: 2455-4855 (Online) ***Review Article***

Received: 11th January, 2017; **Accepted:** 3rd February, 2017; **Published:** 28th February, 2017

Recent progress in organic nano-composites: Synthesis and treatments for use as active layers in electronic devices

Mariem Saoudi[1], Ridha Ajjel[1] and Boubaker Zaidi[2,3*]

[1]Laboratory of Energies and Materials (LabEM), Higher School of Sciences and Technologies of Hammam Sousse, Sousse University, Tunisia; [2]Higher School of Data Processing and Mathematics of Monastir, Technology Department, Monastir University, Tunisia; [3]Department of Physics, Faculty of Sciences Ad-Dwadimi, P.O. Box 1040 Ad-Dwadimi 1191, Shaqra University, Saudi Arabia

***Corresponding author:** boubaker_zaidi@yahoo.fr

Abstract

The present work represents an overview for organic materials and their nano-structuration using carbon nano-tubes. Particular attention is allowed to the polyaniline polymer and single walled carbon nanotubes which are the subject of our theoretical and experimental investigation after their functionalization. In the other hand, we give a detailed report concerning the previously used synthesis methods, incorporating polymers and carbon nanotubes. In fact, the functionalization process needs some technical treatments including purification, nanotubes dispersion and alignment on the organic matrix. Therefore, we give a detailed description of physical and chemical methods used to achieve the functionalization process. Moreover, the aptitude of organic nano-composites for the use as active layers in electronic devices, especially in electroluminescence and photovoltaic conversion is also discussed and evaluated by comparison to those of inorganic conventional semi-conductors. The second section of this present work represents a correlation of experimental and theoretical results obtained in our laboratory on the Polyaniline/ single walled carbon nanotube as a prototype of organic nano-composite. The study is focused on the evaluation of the properties of the charge transfer between both components. In this context, Polyanilineemeraldine base (PANIEB) is doped with sulfonic acid in Dimethyl formamide (DMF) solvent and mechanically functionalized with single walled carbon nanotubes (SWCNTs). A systematic vibrational and optical study is achieved as a function of SWCNTs weight concentration. Also, Fourier transform infrared (FTIR) analysis and optical absorption (OA) measurements were achieved. Our aim is to evaluate the functionnalization process between both components and to elucidate the corresponding changes on the optical properties. In this context and to support the charge transfer from doped polyaniline to carbon nanotubes, analogous theoretical study based on Density Functional Theory (DFT) is carried out. This study is based on the optical and vibrational

calculations. Principally, spin density distribution, atomic charge and bond length modifications from ground to oxidized state are used to supports the grafting process. The correlation structure-properties obtained either experimentally or theoretically evidences that the resulting composite exhibits good photovoltaic properties.

Keywords: Density functional theory, photovoltaic cells, single walled carbon nanotubes.

1. Introduction

Polymer materials exhibit some interesting properties and therefore can be used in a large field of applications. Before the discovery of their photo-conductive properties, polymers are principally used in the packaging industry, in the building, automotive, household appliances, textile, electricity. However, in the last few decades, conductive polymers have attracted considerable interest in use as active layers the electronic organic devices (Burroughes et al*.,* 1990; Saxena et al*.,* 2003; Han et al*.,* 2014). The conductivity of these materials which are insulating at their neutral state, is obtained either by chemical doping or by the addition of conductive elements (Ahllskog et al*.,* 1997). Due to their flexibility, and the easy doping process, these materials offer the advantage of the modular electronic and mechanic properties. In fact, the Nobel Prize for Chemistry was awarded for Shirakawa, Heeger and MacDiarmid for the revolutionary discovery (Heeger*,* 2001) and hence they exhibits some characteristics which are not found in inorganic semiconductors (Wu et al*.,* 2015; Schôn et al*.,* 2001; Razykov et al*.,* 2011). Organic materials are in our days the most promising candidates for the use as active layers in the future of electronic devices manufacturing, due to their interesting electro-optical properties (Lizin, 2012; Deng et al*.*, 2016; Tehrani et al*.,* 2015). As it is widely known, fragility and operating life time are both handicaps for electronic organics devices. To overcome these handicaps, the added small amount of carbon nanotubes leads not only to a good mechanical strength (Moaseri et al*.,* 2014) but also in higher operating life time (Mulligan et al*.,* 2015). Particularly, for photovoltaic applications, the good dispersion of carbon nanotubes in the polymer matrix leads not only to the charge transfer but also to better transport properties via their good electron-hole mobilities (Zhu et al*.,* 2009). This charge transfer occurs because the overlapping between the electron diffusion length and the distance separating the photo-generation sites and nanotubes. Physically, the charge transfer creation involves generally additional absorption features in the visible region and results in a good compatibility with the solar spectrum (Zaidi et al*.,* 2010). In fact, the resulting interpenetrating network results in higher charge separation and good collection efficiencies due to the formation of bulk P-N hetero-nano-junctions (Ferguson et al*.,* 2013;Gao et al*.,* 1995, Janssen et al*.,* 2005).

Among of conducting polymers, polyaniline (PANI) is the most highly studied due to its varied chemical and physical properties (MacDiarmid*,* 1997; Malinauskas, 2001; Hundley et al*.,* 2002). The particular interest restricted to this material is the consequence of good environmental stability and easily synthesis (Huang et al*.,* 2004;Zhangand Wan*,* 2003; Pinto et al*.,*2003; Zhou et al*.,* 2003). A simple chemical treatment of PANI leads to new oxidation degree where its conductivity can be reversibly switched between electrically insulating and conducting forms (Molapo et al*.,* 2012). The fully oxidized (reduced) form is

named as per nigraniline base PNB, (leucoemeraldine base LB). Then, if nitrogen atom is half oxidized, PANI is in emeraldine base form (EB; form) (Aleman et al*.,* 2008).

Although, some systematic studies involving PANI have been published, few papers have been devoted to the possibility of its integration as active layers in photovoltaic devices under its different doped or undoped forms (Bejbouji et al*.,* 2010). Therefore, it is of interest to study the modification of their properties upon acid doping and after its functionnalization with carbon nanotubes. For that and in order to specify the appropriate applications, correlation structure-properties should be established either experimentally or theoretically (Pietro et al*.,*1992; Pickholzand dos Santos*,* 1999; DiCesare et al*.,* 1998; Ayachi et al*.,* 2006; Zouet al*.,* 2009). Indeed, quantum calculations based on density functional theory (DFT) are the most appropriate tools to describe the organic materials properties (DiCesare et al*.,* 1998; Khoshkholgh et al*.,* 2015; Mbarek et al*.,* 2012). These calculations permit to give some information which are experimentally inaccessible and permits to predict the applicability field (Mbarek et al*.,* 2012;Ayachi et al*.,* 2012). Then, as a consequence of data processing development, calculations using large scale basis set and a large number of repeating units are currently possible (Khoshkholgh et al*.,*2015; Mbarek et al*.,* 2012).

In this work after presenting a review concerning organic nanostructures and their applications, a combined experimental and theoretical investigation on the composite based on doped polyaniline and single walled carbon nanotubes (SWCNTs) is presented. Our aim is to establish a correlation structure-properties after carbon nanotubes adding and to evaluate possible applications based on the observed optical and vibrational properties changes. Experimental optical absorption and FTIR measurements are used to evaluate changes on the optical and vibrational properties. Moreover, a systematic theoretical study based on DFT quantum calculations is presented in order to elucidate the polymer functionalization process with SWCNTs and to evaluate the parameter of the photovoltaic cell that can be fabricated from. Particularly, the charge transfer properties and the corresponding electronic structure are of great interest.

In the first section of this paper, a general description of conductive polymers will be presented. Particular attention will be given to the material to be the subject of this work, namely the polyaniline. In the other hand, to make the report easy to read we first present a detailed description of chemical, electrical and optical properties and the corresponding applications reported in the literature. In the second section, we will present the changes of these properties when carbon nanotubes are inserted in the organic matrix. Moreover, a detailed description of the corresponding used procedure, previously reported, which Permits nano-composite obtention, will be also presented Finally, the functionalization process with single walled carbon nanotubes (SWCNTs) and the change of vibrational, optical and electronic properties will be presented. All the obtained results will be restricted for the of use in photovoltaic conversion.

2. Discovery of intrinsic conductive polymers

Starting from the year 1950, the need for small and flexible components required the design of new materials combining the flexibility and modulable electrical and optical properties. These new materials, made of polymers having a high electrical conductivity, are called conductive polymer. The first

conductive polymers have been developed by adding external conductive agents such as iodine (Harigay, 1992), when the conductivity is 10^9 order of magnitude higher than that of intrinsic state. However, conjugated polymers at their neutral states are classed as conductive polymers (Salaneck et al., 1999). Their peculiarity is that they exhibit a single double bond alternation (system π-σ-π) called π-conjugate structures. This network allows electron delocalization along the macromolecular skeleton due to the overlapping of π orbials. Thus, by association of the repetition units, there would be an orbital overlap type of π extended over several atoms.

Polyenic polymers represent the first categories which is constituted only by the repetition of single/double bonds such as poly trans (acetylene) (PA). however, Aromatic polymers are formed by aromatic ring such as poly (para-phenylene) (PPP) note that hetero-atoms can be present on the conjugated aliphatic squeleton such as polyaniline (PANI), for which the structure will be presented in this paper. In the other hand, if the ring contains an hetero atom, the polymer is called heterocyclic aromatic polymers such as poly (thiophene) (PT) or poly (pyrrole) (PPy). Finally for mixed polymers, the structure is constituted by alternating copolymers from the abovementioned groups such as poly (para-phenylenevinylene) (PPV) or poly (parathylenevinylene) (PTV).

3. Oxidized states of polyaniline

Poly (aniline) (PANI) is a polymer, for which the structure is constituted by the repetition of aromatic ring and a nitrogen bridge (Scheme 1), allowing it to exhibit some specific properties. It can be obtained by polymerization from aniline via chemical, electrochemical or enzymatic catalysis (Cholli et al., 2005). PANI can exist in three forms depending on the degree of oxidation of the nitrogen atoms.

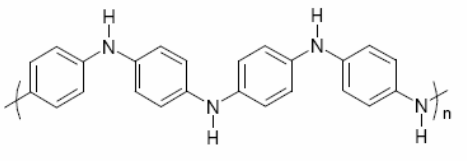

Scheme 1: Chemical structure of polyaniline.

The first form called pernigraniline is a red solid composed of sequences of 100% of oxidized units of the quinonediimine type (Scheme 2). This solid is easily hydrolyzed in an acid medium.

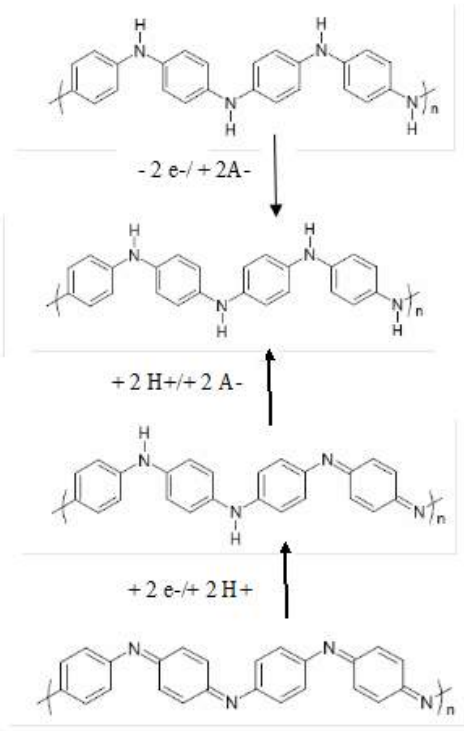

Scheme 2: Polyaniline oxidized forms.

The second form of the polyaniline is blue colored emeraldine , formed by 50% of benzene diamine reduced units and 50% of quinonediimine oxide units. This is the stable form of PANI. The third form is called leucoemeraldine, which is a white solid

composed of a 100% in the reduced state of the benzene diamine moieties. In its emeraldine base form, the PANI is a semiconductor whose the theoretical gap is estimated at 1.4 eV by Vignoloet al., (Vignolo et al*.,* 2001). This value is slightly lower than those measured experimentally, of the order of 2.0 eV (Cao et al*.,* 1989; McCall et al*.,* 1990; Cao*,* 1990; Scully et al*.,* 1993). In contrary, emeraldine salt is the conductive form of PANI which can be obtained by Redox doping of the leucoemeraldine form during chemical or electrochemical oxidation reactions. During redox doping, the number of π electrons changes, while the number of protons remains unchanged. Moreover, the PANI has the particularity of being also doped by interaction with a Lewis acid (Genoud et al*.,* 2000; Kulszewicz-Bajer et al*.,* 1999; Chaudhuri et al*.,* 2001; Dimitriev et al*.,* 2004) when the electronic change is accomplished via of the nitrogen atoms. It can also be doped by simple protonation of the emeraldine base form by a Brönsted acid (Chiang et al*.,* 1986). The emeraldine salt (ES) can be obtained by oxidation of the leucoemeraldine base (LEB) (a), or by protonation of the emeraldine base (EB) (c). The 100% oxidized form is called as pernigraniline base (PNB).

4. Carbon nanotubes: Synthesis, structural, electrical and optical properties

Carbon nanotubes were accidentally discovered by S. Iijima in 1991 (Iijima*,* 1991). when observing Electronic microscopy the secondary products obtained during the electric arc synthesis of fullerene molecules. Carbon nanotubes structures are derived from the fullerene form which form a coiled graphite plane closed on each side by two hemispherical caps.

These carbon nanotubes have diameters of the order of nanometers and lengths varying from a few µm to a few mm. Indeed, they have a very important geometrical factor that gives them a quasi-1D geometry. carbon nanotubes can exists as single-walled carbon nanotubes (SWCNTs) or multi walled carbon nanotubes (MWCNTs).

The MWCTs are composed of concentrated tubes of various diameter ranging from 2 and 50 nm (Fig. 1) The inter-tube distance is 3.44 Å (Ebbesen et al*.,* 1994), a distance close to the distance between graphite planes which is 3.35 Å.

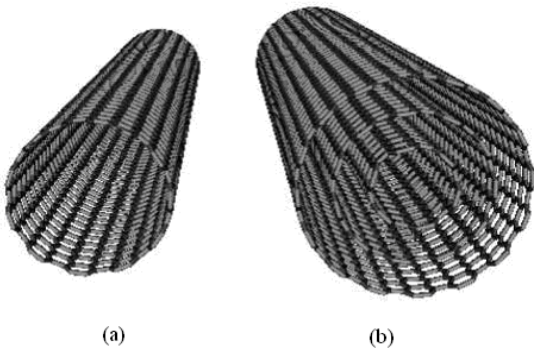

Fig 1. Single-walled carbon nanotube (a) and Multi-walled carbon nanotube (b).

4.1. Single Walled carbon nanotubes SWNTs

These nanotubes are formed by a single sheet of graphene. Because of the cohesive Van der Waals interactions, these nanotubes are grouped as bundled SWCNTs containing a number of 20 to 100 nanotubes and adopt a periodic arrangement of triangular symmetry. Inter-tube distances are in the order of 3.2 Å (Thess et al*.,* 1996). Thus, observation of isolated single-celled nanotubes is not obvious. Moreover, separation and dispersion process should be considered in order to isolate these structures. Due to its analogy with the graphene sheet (sp^2 hybridized carbon atoms network,

Van der Walls interaction, ...), the carbon tube can be described as the enrolment of a graphene plane. This enrolment is carried out by coinciding the two ends of a $\vec{C}_h$ vector defined as equation 1 (Fig. 2)

$$\vec{C}_h = \overrightarrow{OA} = n\vec{a}_1 + m\vec{a}_2 \qquad \text{(Eq. 1)}$$

and the angle θ as follows as summarized in (Eq. 2) and (Eq.3).

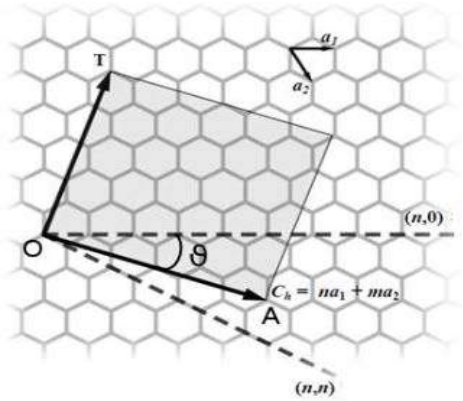

Fig 2. Representation of the vector defining the enrolment of the graphite sheet in order to obtain a single-walled carbon nanotube.

The nanotube axis is perpendicular to the vector and the hexagons form a helical enrolment on the surface of the nanotube. The helicity of the tube depends on the angle θ between a_1 and $\vec{C}_h$, called the chirality angle. Then, depending on the angle θ for which value are is between 0^0 and 30^0, there are several ways to form the tube. If θ = 30^0, n = m: the nanotube consists of hexagons parallel to the tube axis. The structure is called "armchair" type (Fig. 3a). then, if θ = 0^0, n = 0 or m = 0: the nanotube seems to possess a hexagon belt in the plane perpendicular to its axis. The structure is the "zig-zag" type (Fig. 3-b). However, if 0^0<θ<30^0, n = m = 6, All other possibilities. Their enrolment forms an Archimedes screw, the structure is the "chiral" type (Fig. 3-c). According to the Euler law 6 pentagons are sufficient to form the cap which closes the nanotube. The type or chirality of the nanotube, defined by its pair of index (n, m) is an essential parameter to modulate its properties. Based on the distance $a_{C\text{-}C}$ between carbon atoms in the tubes which is nearly 1.42 Å, we can deduce the diameter d of the tube

$$d = a_{cc}\frac{\sqrt{3(n^2 + nm + m^2)}}{\pi} \qquad \text{(Eq.2)}$$

$$\theta = arctg\left(\frac{m\sqrt{3}}{m+2n}\right) \qquad \text{(Eq.3)}$$

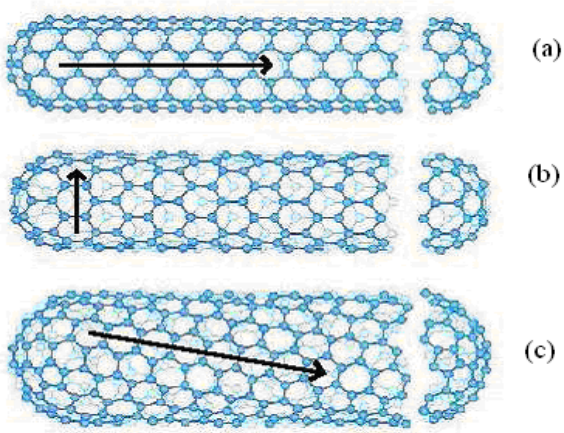

Fig3. Different types of nanotube structure: (a) armachair (n = m), (b), zigzag (n, 0) and (c) chiral (n≠m).

4.2. Production methods

Different methods of synthesis are intensively made where the properties of the resulting product is severely controlled in terms of diameter, and the number of concentric walls

for Multi-walled carbon nanotubes. Depending on the temperature, there are two different processes to synthesize carbon nanotubes. For the high temperature processes (temperatures above 3000^0C) there are two methods such as electric arc (IIjima, 1991; Journet et al., 1997) and laser ablation (Guo et al., 1995). Similarly to the medium temperature processes (temperatures below 1000^0C), there are two methods which are respectively the catalytic decomposition (Kitiyanan et al., 2000) and the PECVD (plasma enhanced chemical vapor deposition) (Gohier et al., 2007).

4.3 Nanotubes obtained electric arc technique

The electric arcis established between two graphite electrodes located in a reactor filled with an inert gas such as helium or argon. The temperature elevation permits the graphite sublimation. A condensation process is established on the end of the cathode which results on the formation of nanotubes. If the anode is a pure graphite, multi-walled nanotubes will be formed. However, in the presence of metal catalysts, single walled will be synthesized (Journet et al., 1997; Iijima and Ichihashi, 1993). The synthesized nanotubes have few structural defects but are generally polluted by numerous impurities (catalyst, amorphous carbon).

4.4. HiPCO method for nanotube production

The HiPCO process (High Pressure Carbon monoxide) is a catalytic decomposition method (Bronikowski et al., 2001). A flux of monoxide carbon CO is injected with Fe(CO)5 particles in a high pressure furnace (10 atm) for which temperature is ranged between 700^0C and 1200^0C. The iron particles play the role of catalyst and allow the nucleation of carbon nanotubes (Eq.4).

$$CO\ (g) + CO\ (g) \rightarrow C\ (s) + CO2 \qquad \text{(Eq.4)}$$

For his method, the formation SWNTs is favored. Despite the SWCNTs geometry is nearly uniform (mean diameter of 0.8 nm), nanotubes are less graphitized than those achieved by the electric arc method.

4.5. Nanotube obtianed by CoMoCAT method

The CoMoCAT method (Cobalt Molybdenum CATalytic method) is also a method of catalytic decomposition which uses a Cobalt/Molybdenum mixture as a catalyst (Kitiyanan et al., 2000). It operates at temperatures between 700^0C and 950^0C and a pressures between 1 and 10 atm. This technique allows a good control on the characteristics of the resulting SWCNTs by changing synthetic parameters such as Mo/CO fraction, temperature or reaction time (Kitiyanan et al., 2001).

4.6. Properties of carbon nanotubes

4.6.1. Electronic and optical properties

The electronic properties of carbon nanotubes are essentially made from the structure of a graphene sheet. As it is known, the graphene is a semiconductor with a null optical gap from which Fermi surface is summarized by 6 states, providing the energy overlapping between both valence and conduction bands. This means that only 6 states (k_x; k_y) are responsible for conduction in the graphene plane. The enrolment of the graphene sheet to form SWCNTs, is accompanied by the appearance of new conditions periodic limits. These new limit conditions results in the quantification of the wave vector $\vec{k}$ in the enrolment direction, as in the following expression (Eq. 5).

$$K = \frac{n * \pi}{d} \quad \text{(Eq.5)}$$

Thus, the nanotube can be conductive if one from the 6 states (kx; ky) corresponds tothe quantification condition imposed by the limit conditions. In all other cases, the nanotubes are semiconductors. Therefore, the electronic properties of CNT depend on the integers n and m which definite chirality (Saito et al*.,* 1992). Indeed, the nanotube is conductive if the following condition is satisfied (Eq. 6).

$$n - m = 3P\,,\ (n, m, P) \in N^3 \quad \text{(Eq.6)}$$

The density of states of the carbon nanotubes diverges for some energy values so-called Van Hove singularities, typical for uni-dimensional structure. For nanotubes, electron transitions take place between these singularities, For the first transition E_{11}, the energy of the gap can be expressed by Eq.7, Where $a_{C\text{-}C}$ = 1.42 Å, distance between carbon atoms E_0 = 2.9 eV, interaction energy between two neighboring carbon atoms.

$$E_{11} = \frac{6a_{C-C} * E_0}{d_{NTC}} \quad \text{(Eq.7)}$$

The electronic properties of CNTs can be modified by charge transfer. The carbon nanotube can be p-doped by substitution where carbon atom is changed by boron atom. The n-doping process can be accomplished by substituting the carbon atom with a nitrogen atom. Doping process can also take place by surface adsorption of electron donating or accepting species such as alkali metals, halogens (Lee et al*.,* 1997) or organic molecules.

Carbon nanotubes are good conductors (higher conductivity than copper). They are very good models for ballistic transport, demonstrated experimentally for SWNTs by Kong et al. (Kong et al*.,* 2001). Carbon nanotubes can support high current densities (higher than that of copper) typically 107 A/cm2 (Franck et al*.,* 1998). CNT are also good super conductors at lower temperature.

4.6.2.Mechanical properties

CNTs possess single/double bonds alternation which give the structure a high mechanical strength. Thus, the Young Modulus values obtained for either SWNTs, or MWNTs, are in the order of 1 TPa (Salvetat et al*.,* 1999). However, these values are strongly dependent on the structure of the resulting material (principally the presence of defects) and can be decreased to 10GP (Salvetat et al*.,* 1999). The nanotubes also have a high deformation capacity and a high flexibility which allows reversible deformations. This flexibility is due to a strong sp^2-sp^3 re-hybridization of the carbon atoms. The breaking strength is also very high, typically between 13 and 52 GPa which is in the same order for steel 200 MPa (Yu et al*.,* 2000).

4.6.3. Thermal properties

Thermal conductivity measurements carried out on the SWNTs show that thermal conductivities varies from 1800 to 6000 W: K^{-1}: m^{-1} (Kimand and Jin*,* 2001; Hone, 1999) higher than that of diamond (2000 W: K^{-1}: m^{-1}). These values are strongly dependent on the orientation of the tubes during the measurement.

4.6.4. Optical properties

The black color of carbon nanotubes is indicator of their high optical absorption in the areas of the UV-visible-near IR (Yang et al*.,* 2008). Carbon nanotubes also have electro-luminescence properties that allow them to emit in the infrared frequencies (Freitag et al*.,*

2004) as well as good photoconductivity properties (Shim et al., 2003; Stewart et al., 2005; Lu et al., 2006). They also possess photoluminescence properties as demonstrated by O'connell et al., (O'Connell et al., 2002).

5. CNTs / PANI Interaction

The functionalization of carbon nanotubes with polyaniline can results from π-π interactions or covalent bonding. The untreated nanotubes generally result in non-covalent bonds between the C = C bonds and the aromatic rings of the polymer (Scheme 3). On the other hand, if CNTs are treated with a strong acid such as the COOH groups, covalent bonding between both components is the most preponderant exchange protocol. Mixing the properties of nanotubes with those of conductive polymers, mainly polyaniline, represent recent investigation field.

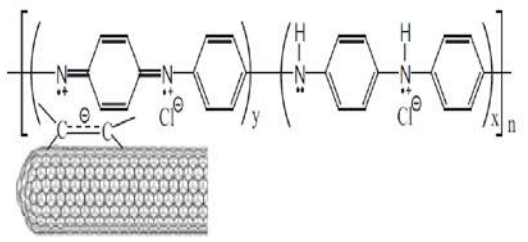

Scheme 3: Interaction of π-πtype between CNTs and polyaniline.

6. Functionalization of carbon nanotubes with polymers

6.1. Purification and separation of carbon nanotubes

After the synthesis of the carbon nanotubes, the final product contains residual impurities related to the synthesis protocol (amorphous carbon, catalyst particles, impurities). These impurities lead to undesirable effects on the electronic properties of the nanotubes and / or the obtained composites. Therefore, purification process are needed after carbon nanotubes synthesis. Several methods are previously reported to have a better purity such as chemical methods, based on the selective oxidation process (Zhang and Wan, 2003). However, physical methods are based on filtration (Bonard et al., 1997) and centrifugation (Hu et al., 2005). It should be noted that generally some techniques should be combined to purify CNT, for which, chemical and physical techniques must be coupled (Wang et al., 2006). Moreover, for all synthesis methods, nanotubes were found in both single and mullti-walled forms.

As it is mentioned both categories differs by electronic and optical properties and present an handicap for applications (mixing between metallic and semiconducting nanotubes). To ensure separation, a technique based on gradient of density ultracentrifugation was generally applied. A better separation process between both categories is strictly based on differentiation of their diameter (Arnold et al., 2006). This method selectively separates small and large diameter tubes (Arnold et al., 2005).
The selection by non-covalent interactions with a conjugated polymer via a functionalization process in acid medium (Strano et al., 2003) was also used. Other ways such as selection by interaction with DNA wrapping (Zheng et al., 2003) or by di-electrophoresis technique (Krupke et al., 2003) have also been tested. These three techniques allow the selection of carbon nanotubes in liquid phase.

6.2. Dispersion of carbon nanotubes

After the purification process and in order to obtain a good nano-composite, CNTs should be homogenously distributed in the organic matrix. In this context, it is currently known that the good dispersion of CNTs in polymer matrix is

the major step which leads to good exploit of their properties. Thus carbon nanotubes exhibit strong cohesive interactions of Van der Waals type. These interactions induce strong aggregates of several micrometers in diameter, randomly distributed (Fig.4). Such an arrangement can not induces any specific properties on the final nano-composite.

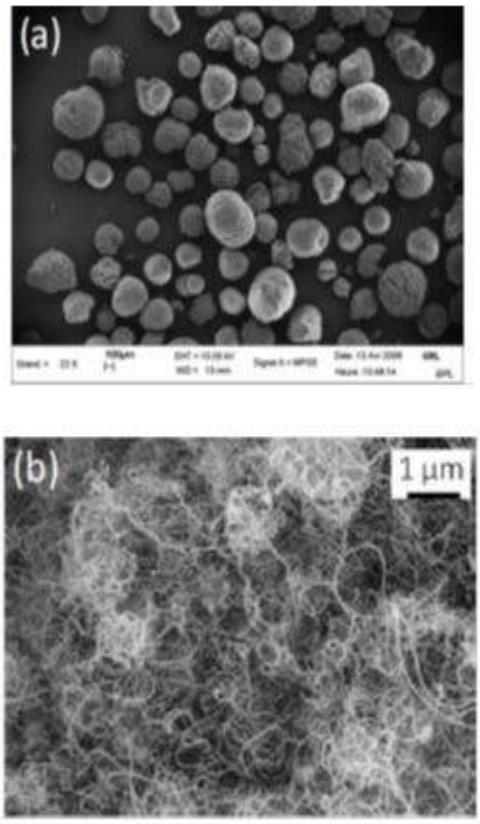

Fig 4. Structure of bundled CNT (a & b).

To achieve good dispersion process, for which carbon nanotubes should be uniformly distributed in the polymers matrix, some techniques are recently used. It should be noted that these techniques are essentially made to separate tubes without destruction of the its structural integrity. In the last decades, intensive efforts have been focused to improve the CNTs dispersion on the polymer matrix. The easiest method is the direct mixing of CNTs with the polymer. The chemical modification of the polymer matrix or of the surface of the CNTs was also applied. These approaches are aimed to approach affinities values of both components. It is also possible to use a third element, such as surfactants.

6.2.1. Direct Mixing Method (Mechanical Method)

In general, during mechanical agitation, the local force induced by vibration decomposes CNTS aggregates. The complete separation of the CNTs aggregates requires an energy (mechanical or vibrational) greater than the binding energy of the Van der Waals cohesive forces. This can be accomplished in low-viscosity solvents, such as water and organic solvents (Huangand Terentjev, 2012). It is a simple method based on the use of mechanical agitation or vibration forces. An intense agitation (14000-18000 rpm) of the CNTs for a well-defined time allows a better dispersion process (Alimi et al., 2011; Sandler et al., 1999). On the other hand, it is demonstrated that when the agitation is followed by ultrasound with controlled frequency and power, makes it possible to have nano-composites of high qualities (Park et al., 2008). Chen and all. showed centrifugal forces applied in the nano-composite result in better homogeneity and alignment of CNTs (Chen et al., 2007). It should be noted out that this method, which uses intense vibratory forces, can give rise to breaks in tubes which imposes changes on their properties (Kerr et al., 2011). Indeed, it is clearly seen that longer agitation time induces change on the length distribution.

6.2.2. CNTs surface modification

CNTs surface modification is based on the its chemical functionalization through covalent bonding with functional groups. The process can also be governed with non-covalent bonding between CNTs and molecules (Moradi et al*.,* 2012; Liu et al*.,* 2012) (Fig.5).

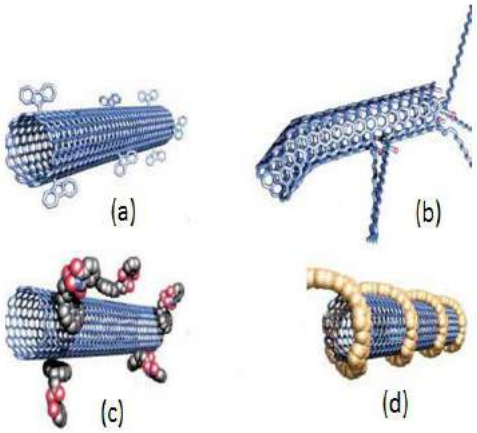

Fig 5. Surface modification of CNTs: (a, b) covalent bonds, (c, d) non-covalent bonds (Airsch **et al., 2002).**

6.2.2.1. Chemical functionalization

The chemical functionalization can be carried out either by organic chemical reactions or by reactions induced after creating structural defects of CNTs. In this context, CNTs can be functionalized using special reactive groups, such nitrenes (Holzinger et al*.,* 2004), lithium alkyls (Viswanathan, 2003), fluorine radicals (Peng et al*.,* 2003; Mickelson et al*.,* 1998). After surface modification, it is easy to graft functional groups such carboxylic acid, hydroxy or amine type on the surfaces of CNTs, allowing the formation of covalent bonding with polymers or with molecules (Martín et al*.,* 2012). The multi-walled carbon nanotubes were previousely oxidized with inorganic acid by Gojny et al (Gojny et al*.,* 2003) for which transmission electron microscopy results showed a good incorporation in an epoxy matrix. It is also poosible to accomplish the polymerization process after the chemical functionnalization. The approach consists first in linking the functional group on the surface of the tubes and then, the of polymerization process take place (Shanmugharaj et al*.,* 2007; Qin et al*.,* 2004).

6.2.2.2. Physical functionalization

This approach consists to create non-covalent interactions between CNTs and the molecules chosen to be functionalized. It has been demonstrated that adding some functional groups such as pyrenes (Vijayakumar et al*.,* 2011), anilines (Rajarajeswari et al*.,* 2012), and amines (Kong et al*.,* 2001) leads to a good dispersion of CNTs in organic solvents. In this case and due to the weak interaction between CNTs and molecules the electronic properties of the original materials are conserved.

The process can be also carried out by in situ polymerization, as it is previously described by Deng et al (Deng et al*.,* 2002),when synthesizing polyaniline/CNTs nano-composite. All component of the mixture were added with stirring in a very specific amount in order to reach an effective system stabilization.

Fig.6 depicts the functionnalization process of MWCNTCs / polypyrrole composite (Sahoo et al*.,* 2007). The CNTs were treated with an acid and the polyperrole was then functionalized by chemical polymerization in situ using iron chloride $FeCl_3/6H_2O$ as an oxidant. It has been demonstrated, that the COOH groups interact via non-covalent bonding simultaneously with both C=C bonds of CNTs and the N-H groups of the polypyrrole (Fig. 6).

Morishita et al., (2010) have also obtain a good dispersion of SWCNTs when using

polymalein (MIP) in several organic solvents. Results showed an homogeneous solubilization of CNTs within the polymer matrix widh improved the physical properties relative to the resulting composite.

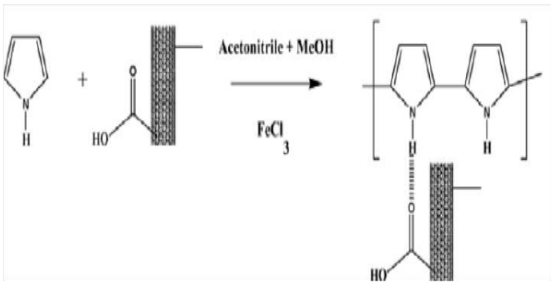

Fig 6. Interaction between polypyrrole and multi-walled CNTs.

For all adopted method, the stability of the obtained solutions, especially concerning the dispersion process, is of short duration and consequently CNTs rapidly agglomerate on the surface of the solution. The use of ultrasonic baths to separate aggregates represents a good adopted solution. However, frequencies and energy should be controlled in order to evitate the nanotubes degradation (Kerr et al*.,* 2011).

6.3. Orientation of carbon nanotubes in the polymer matrix

The performance organic electronic devices using CNTs embedded on the polymer matrix is strongly dependent on their CNT orientation. Physically, for optoelectronic applications, oriented nanotubes permits charge transport and reinforces the optical properties in a preferential direction so called spatial anisotropy. To achieve good CNTs orientation, two ways are used. The first consists to orient CNTs during their synthesis, whereas for the second one (the most used), the alignment process is done the liquid phase after the synthesis by Applying external perturbations.

6.3.1. CNTs Orientation during synthesis

Using vapor deposition (CVD) technique (Fig. 7), metallic catalyst nanoparticles (Fe, Ni, Co, Mo) permit to obtain CNTs vertically aligned with the substrate (Futaba et al*.,* 2004). In fact, the high density of CNTs is the principal factor which favors good orientation. Moreover, it is also possible to apply an electric field during the growth, which allows to improve their alignment (Meyyappan et al*.,* 2003). It should be noted that the most efficient alignment can be achieved during the synthesis step. However its complexity is originated from dyamic structural changes (Rarvikar et al*,*2005, Boncel, 2011).

6.3.2.CNTs Orientation after the synthesis

Among of the widely used methods is the liquid phase after the CNTs dispersion. This method is based on the application of external perturbations such as an electric field (Chen et al*.,*2001; Domingues et al*.,* 2012) or magnetic field (Hone et al*.,* 2000; Choi et al*.,* 2003).

It is also possible to use light excitation which permits elastic movement CNTs as it is previously reported for SWCNTs (Zhangand Iijima*,*1999). Several experimental and theoretical studies relative to the orientation of single- or muti- walled nanotubes via electric or magnetic fields applications are reported on the literature. The application of electric field between two electrodes, leads to orientate nanotubes parallel to their intrinsic dipolar moments (Dimaki et al*.,* 2004).

Park et al*.,*(2006) have study the field effect on the degree of SWCNTs alignment of SWCNTs. They have shown that the electrical conductivity and the dielectric properties of the nano-composite can be modulated by varying

the characteristics of the electric field (amplitude, frequency, time).

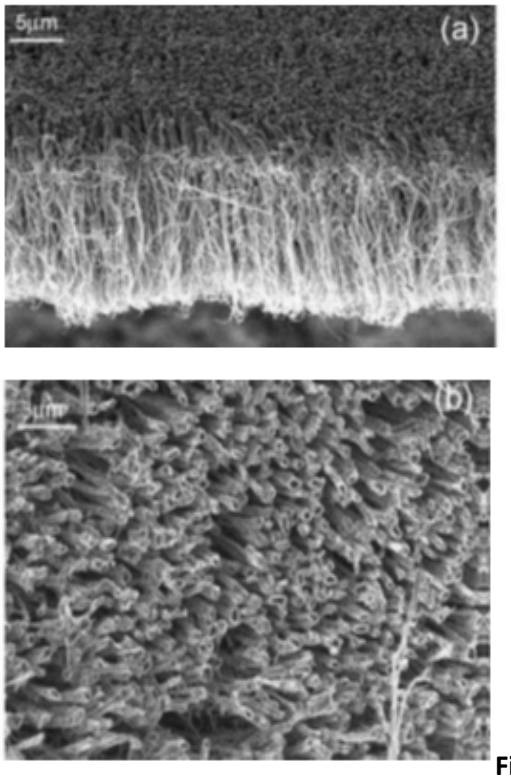

Fig 7. CNTs Alignment (a) lateral vision, (b) longitudinal vision (Chen, 2005).

The application of the electric field creates a dipole moment, and the resultant force induces the tube in the field direction (Fig. 8.a). Moreover, the oriented carbon nanotubes interact with each other as dipole-dipole interactions as illustrated in Fig. 8.b. these effects are responsible for their movement to form an oriented networks connected in "head-to-head" (Fig.8.c). In the other hand, it has been demonstrated that moderate annealing treatment, induces a higher electric photocurrent in photovoltaic solar cells (Yang et al*.,* 2005; Savenije et al*.,* 2006). This amelioration has been interpreted as good arrangement of polymer and CNTs at the molecular scale (Zhokhavets et al*.,* 2006).

It should be noted that CNTs orientation process in the organic matrix, can induce polymer alterations, mainly the decrease of conjugation degree, which modify its electronic properties. Moreover, the orientation process can induce modifications on the polymer structure.

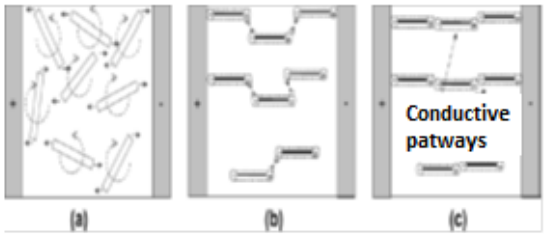

Fig 8. CNTs orientation process by application of electric field (a): orientation in the direction of the field (b): head-to-head interaction and (c): formation of the network (Monti, 2012).

7. Applications in the organic electronic devices

7.1. Electroluminescence of organic materials

Electrical excitation induces excitons creation for which the diffusion length is typically in the order of few nanometers. Depending on its spins, exit on can be singlet or triplets. The singlet de-excitation is accompanied by a radioactive decay, however, triplets involves non-radioactive decay process. Depending on the nature of the molecule, the created exciton can be either Frenkel type (electron-hole strongly bound: El ~ 1 eV) or of Waner type (electron-hole weakly bonded El ~ 0.1 eV). Another type of exciton may exist in organic structures namely, the charge transfer exciton

(CTE). The latter is an intermediate case between the two previous systems which are largely reported for in inorganic semi-conductors. CTE describes a system where the exciton is delocalized through several repeating unit of a polymer, due to their anisotropic nature. Currently, the degradation processes, mainly residual carbonyl groups and/or the interaction of the electrodes with air are levitated, using the concept of encapsulation with transparent glass. The encapsulated ITO / PPV / Ca luminescent device showed a very good stability when operating in air for 7000h and at 20^0C (Carter et al*.,* 1997). The range of products of commercial interest have proven a progressive need and the companies like Kodak, Philips, Toshiba, Seiko-Epson are interested to the use of organic materials. In the display screens, the conversion efficiency under operating voltages varying from 3 to 5V is a few tens of Lm/m^2. For Inorganic Semiconductors, except for AlGaInP, the same orders of magnitude were obtained (Kovac et al*.,* 2003). It is also known that the original properties of these materials leads to a spectral luminescence which can cover the entire visible spectrum, by simply modifying the molecular structure. Thus, according to their advantages, namely lower cost and flexibility, organic materials will cover the market for flat panel displays (Mbarek et al*.,* 2012).

As for inorganic semiconductors, the conversion efficiencies are also dependent on the molecular structure and the architecture of the component. Currently, the some works are focused on the realization of low cost consumable components with higher performance. For the conjugated polymers, one of the methods is to introduce a conjugation interruption which favors a radioactive channel resulting from of excitons confinement.

7.2. photovoltaic conversion from organic materials

Due to the need of electrical energy, photovoltaic production is currently a necessity. Fig.9 shows the global evolution of solar energy production over the last two decades (Razykov et al*.,*2011). This production, which reflects our needs is the consequence of various manufacturing technologies which use new materials as active layers.

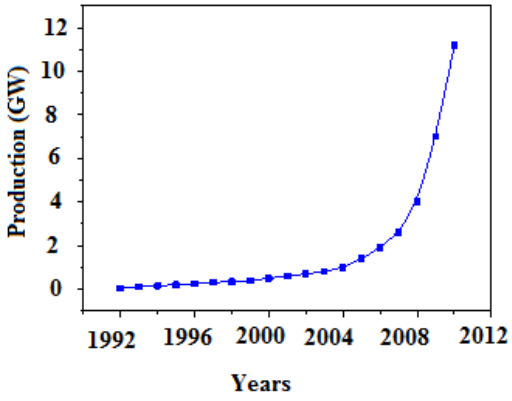

Fig 9. Evolution of photovoltaic energy production in the wide.

The photovoltaic effect has been observed for organic materials for over 40 years. The first organic solar cells exhibited very low energy conversion efficiency (10^{-5}%). Starting from 1986 (Tang*,* 1986). The conversion efficiency reached 1% with the few years ago, this value was reproduced with different materials but never improved. In the beginning of this century, conversion efficiency have started to increase again, reaching 2.5% with the works published by Shaheen (Shaheen 2001), 3.6% with those of Peumans (Peumansand Forrest*,* 2001) under power illumination of 100 mW.cm^{-2} and finally 4.2% with a double heterostructure of C_{60} and copper phthalocyanine (Xue et al*.,*

2004). The record is broken by recent works, using the compound obtained using the hybrid carbon nanotubes/polymers from which CE exceeds 5%. This value is still low when compared to those obtained with mono-crystalline (24.7%) or polycrystalline (19.8%) and amorphous (12.7%) silicon cells (Razykov et al.,2011) (Fig. 10). However, design and production steps are more expensive for inorganic conventional semi-conducting materials (Razykov et al., 2011).

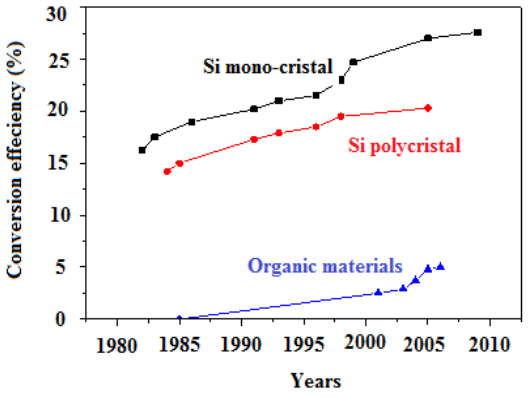

Fig 10. Evolution of photovoltaic conversion efficiencies for silicon (single and poly crystal) and organic materials.

Solar cells based on organic polymers constitute another alternative to those based on inorganic semiconductors, for several advantages. Indeed, these materials offer easy processing, flexibility, lightness and low cost of production. A major handicap is the low mobility of charge carriers (10^{-1} to 10^{-4} cm^2V^{-1} s^{-1}) which remains lower than that that of polycrystalline silicon (50 -100 cm^2V^{-1} s^{-1}) or of silicon single crystal (300-900 cm^2V^{-1} s^{-1}). This mobility handicap can be overcome by using CNTs. Charge carriers motilities of these carbon structures are better than those of silicon ($\mu n \approx 10^6$ cm^2V^{-1} s^{-1}, $\mu p \approx 10^3$ cm^2V^{-1} s^{-1}) (Hongwe et al., 2009). Carbon nanotubes in their single- or multi-walled forms are also characterized by very high rigidity and excellent chemical stability. The addition of a small quantity of CNTs results not only in good mechanical strength but also in the optical gap suitable for the solar spectrum (UV-V range). By their presence, the number of nano-P-N- junctions are maximized and the photo-generated exciton would be able to diffuse where its dissociation occurs at the interface. The distance which separate photo-generation and dissociation sites will be in the order of diffusion length (not exceed 20 nm). Moreover, if the charge transfer is established, CNTs can collect and carry these charge towards electrodes. Prototypes of organic photovoltaic cells have recently been developed, showing a good improvement open circuit currents due to the addition of very low weight fractions of NTCs. The open-circuit currents obtained under illumination of 100 mW/cm^2 vary from 10 to 25 mA / cm^2 (Yun et al., 2008, Derbal-Habak et al., 2011; Jun et al., 2012; Rajiv et al., 2010).

The process of exciton dissociation can be further improved when photo-generation sites are distributed in the bulk. Such a configuration is obtained by organizing donor/acceptor materials in interpenetrating networks, which increase the nano-junction surface. Moreover, the organization of the materials in interpenetrating networks ensures a better charge transfer. Finally, the addition of a small quantity of CNTs to this acceptor/donor hetero-nano-junction is the consequence of better charges collection.

8. Functionalization of SWCNTs with polyaniline: Theoretical and experimental study

As presented in the literature concerning nano-composites and their methods of production, the aims of this work to synthesize

CNTS/ polyaniline nano-composite with simple methods. In the first step the work is focused to obtain better dispersion process of CNTs within the polymer matrix and then to ensure a good orientation of the tubes in a preferential direction. The final objective of this work is to identify the field of application when mixing properties of polyaniline those of CNTs. Finally, we try to use this nano-composite as an active layer for photovoltaic cells.

8.1. Materials and methods

8.1.1. Preparation of the nano-composite

Polyaniline emeraldine base and single walled carbon nanotubes were purchased from Sigma-Aldrich. The polyaniline powder (purity of 99.99%) has the number average molecular weight of Mn > 15000 and a refractive index of 1.85, a melting point higher than 600 K, and a density of 1.36 g/ml at 300K. Then, the SWCNTs were produced by electric arc technique and have diameter varying from 1.0 nm to 1.2 nm and a length of nearly 500 nm. The classical procedure used for the doping process is similar to that previously reported by A. G. MacDiarmid et al. (Chiang et al*.,* 1986). First, the powder was placed for 2 hr in a mixture made up of 20% of sulfonic acid (R-SO3H) and 80% of DMF. Then, the doped polyaniline powder was washed three times by DMF. In fact, treating polyaniline with sulfonic acid having the morality of 1.0, is principally done in order to obtain the conducting form of polyaniline (emeraldine salt) and to facilate the grafting process between both components.

The procedure used to prepare the composite is based on the direct mixture of both components as it is previously described (Zaidi et al*.,* 2010). The PANI at doped states is dissolved in DMF solvent and SWNTs are mechanically dispersed in the same solvent for three hours in two separate recipients. This step is immediately followed by a sonication process for 30 min and by applying centrifuges forces. When the SWCNTs dispersion is achieved, the polyaniline solution is progressively added by a quantitative amount to the already dispersed SWCNTs in order to obtain the appropriate SWCNTs weight concentration. After SWCNTs dispersion, five SWCNTs weight concentrations are obtained (0%, 0.71%, 1.16 %, 2.1 %, and 5 %). These concentrations are chosen to be lower than 5%, principally to overcome Van der Walls cohesive forces in order to obtain a good dispersed SWCNTs state (Byron et al*.,* 2006; Schroder et al*.,* 2003). The obtained solution relative to each SWCNTs concentrations were deposited at room temperature with nearly uniform thickness on silica and KBr pellets respectively for optical absorption and infrared analysis. For optical absorption measurements, all substrates were cleaned in ultrasonically bath with deionizer water and ethanol. The composite film obtained after solvent evaporation is introduced in an oven and is subsequently heated under vacuum at the temperature of 390 K for about 1 h.

8.1.2. Experimental measurements

Infrared absorption measurements are recorded using a Bruker Vertox 80 V interferometer with the resolution of 4 cm^{-1}. The samples were pellets of KBr painted with the organic compound under study (Zaidi et al*.,* 2003). For each SWCNTs weight concentration and in order to eliminate the effect of residual solvent and the KBr, the reference of measurement is obtained by carrying out both infrared spectrum of the KBr alone and those of KBr mixed with the DMF. The optical absorption spectra are recorded using UV1800 spectrophotometer working in the absorption mode with the wave length varying from 200 nm (6.2 eV) to 2000 nm (0.62 eV).

8.1.3. Theoretical details

Concerning the theoretical part, all the structures including PANI at neutral or doped states and at different chain lengths, SWCNTs and the resulting nano-composite have been fully optimized using the most popular Becke's three-parameter hybrid functional, B_3 (Becke et al., 1993), with non-local correlation of Lee–Yang–Parr, LYP, abbreviated as B3LYP method (Pokrop et al., 2009; Leeet al., 1988) without constraint. Theoretically, the PANI doping process is accomplished by adding (removing) electrons to (from) the corresponding modeling structure at its neutral state. For the polyaniline at both neutral or doped state calculations are done for different chain length (the fragments number i (atoms labeled from 0 to 7i in scheme 4). Optical absorption spectra were calculated using the time-dependent density functional theory (TD-DFT) method with the 6-31G (d) basis set which is widely applied to organic polymers (Leeet al., 1988; Gorelsky et al., 2009; Bourass et al., 2016; El Malki et al., 2011; Zhou et al., 2004) and were fitted to Gaussian curves within Swizard program (Gorelsky et al., 2009). Vibration frequencies calculations have been carried out with DFT at 6-31G* level method (Ayachi et al., 2012; Bourass et al., 2016; El Malki et al., 2011) after the ground state optimization. The Highest Occupied Molecular Orbital (HOMO), the Lowest Unoccupied Molecular Orbital (LUMO) levels and the HOMO–LUMO gap are deduced from these calculations (Zhou et al., 2004). The electron density iso-contours plots at the ground states are obtained by the optimization using TD-B3LYP6-31G (d) method. These calculations were performed by the Gaussian 09 package (Frisch et al., 2009).

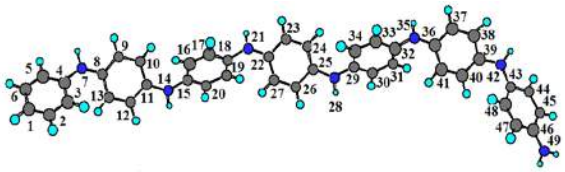

Scheme 4: Molecular structure of polyaniline. Nitrogen (7, 14, 21, 28, 35, 42 and 49) and Carbon atoms are labeled with their number for the optimization in both neutral and doped states.

8.2. Results and discussions

Fig.11 represents changes of FTIR spectra of PANI/SWCNTs composites as a function of SWCNTs weight concentration. Band positions and assignments are referred to the already published vibration studies (Mishraand Tandon., 2009, Baibarac et al., 2003). All spectra are normalized by referring to the band at 1124 cm^{-1} which represent ring deformation and have not been affected when SWCNTs are added.

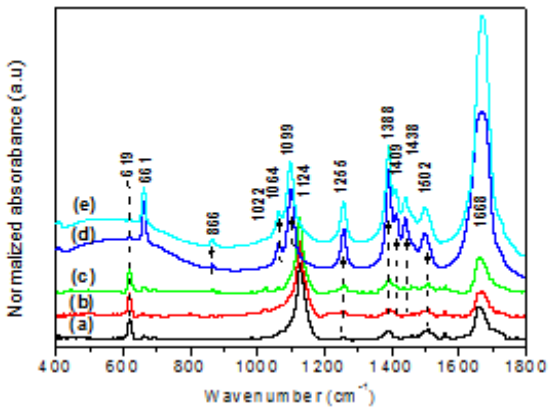

Fig 11. FTIR Spectra of polyaniline functionalized with SWCNTs as a function of SWCNTs concentration (a) 0%, (b) 0.71%, (c) 1.16 %, (d) 2.1 %, and (e) 5 %.

For SWCNTs concentrations lower than 2.10%, there are no significant changes in the shape of FTIR spectra, at least the increase of the band situated at 619 cm^{-1}, attributed to the

C-N deformation. At these concentrations there is a conformational change due to SWCNTs inserting but without covalent functionalization process. Starting from 2.1 % SWCNTs weight concentration, the spectrum is severely affected. New band appears at 1255 cm^{-1}, traducing the covalent binding between both components. Moreover, both bands at 1124 cm^{-1} and at 619 cm^{-1} are respectively shifted to 1099 cm^{-1} and to 661 cm^{-1}. These oscillations frequencies shifts and the netter intensity increase of the last band at 661 cm^{-1}, indicate a new molecular arrangement due to the SWCNTs inserting (Pal et al*.,* 2016).

In the other hand, the weak band situated at 1022 cm^{-1} ascribed to the C-H deformation disappears and a news band appears at 1062 cm^{-1}. Then, bands situated in the range 1350 to 1700 cm-1 are severely affected by referring to those relative to the basic material. Indeed, bands at 1388 cm^{-1} and at 1502 cm^{-1} and 1688 cm^{-1} respectively attributed to C-H binding, ring deformation and N-H switching are dramatically improved in intensity supporting the aromaticity increase of the resulting compound. Two other new bands appear at 1409 and at 1438 cm^{-1} which traduce covalent binding between both components via new C-N link (Lu et al*.,* 2016). In fact, the appearing of new vibration frequencies and the disappearing of another demonstrate that there is a covalent functionalization process (Cosnier et al*.,* 2008). It is of importance investigate this functionalization process which is the major factor to evidence to electro-optical properties of the resulting composite. As carbon nanotubes are generally donating moieties, if there is a covalent functionalization process, polyaniline at doped state will be oxidized. For these reason a re-optimization process and the same calculations are done on the already optimized doped polyaniline structure to reach the oxidized state. Starting from this point of view, fig.12 represents the normalized infrared spectra obtained either experimentally or theoretically of the doped state by referring to those of oxidized state.

In fact, these theoretical calculations are done to support in a first step the molecular structure of the basic material and to elucidate the change from neutral to the oxidized state which can check the reactive sites for an eventual grafting process (Zaidi et al*.,* 2010). Indeed, from the experimental to the theoretical spectrum, all vibrational frequencies are found with nearly same intensities and positions except a shifting of maximum 90 cm^{-1} is observed for the band at 1124 cm^{-1} which represent ring deformation. This shifting is essentially due to the fact that calculations are done in gaseous phases and without inter-chain interactions (Zaidi et al*.,* 2010).

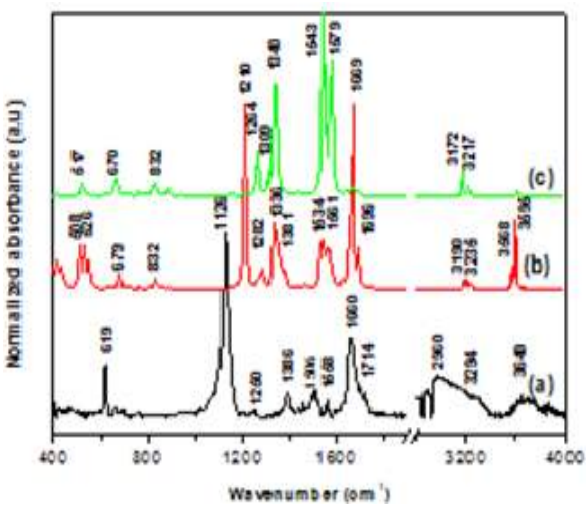

Fig 12. Infrared spectra of doped polyaniline, (a) experimental, (b) theoretical and (c) doped polyaniline after oxidation (c).

Particularly, hindrance effects which are necessarily dominant in the real material are evidently absent on the modeling structure reported in scheme 4, especially for the ring

deformation that appears at 1124 cm^{-1}. From doped polyaniline to its oxidized state there are some changes. First, bands at 1207 cm^{-1} (ring vibration) and at 1667 cm^{-1} (NH_2-switcghing) disappear simultaneously with the appearance of a new band at 1309 cm^{-1}. In the other hand, bands at 1543 and at 1570 cm^{-1} attributed to the symmetric and anti-symmetric C-H binding are improved similarly to those situated at 3190 cm^{-1} and at 3217 cm^{-1}. However, the band at 3595 cm^{-1} is severely quenched. These changes are principally due to the creation of quinoidal form of polyaniline (Mishraand Tandon*.*, 2009; Wang et al*.*, 2016).

Fig.13 represents bond length, atomic charges modifications from the neutral to the oxidized states and the resulting spin density. Atoms are numbered in scheme 4, and bond length number n represents distance between neighboring atoms n and n+1. As shown, for the bond length variations, the most changes are nearly repetitive and concerns bonds which are directly related to the nitrogen atom and/or to their directly bonded carbon atoms.

In fact the oxidation process is followed by a new electronic repartition due to the new conformation as it is represented in fig. 13 which induces the appearing of quinoidal form (Mishra et al*.*, 2009). As shown, before the oxidation process, the higher atomic charges are restricted to nitrogen atoms numbered as 7, 14, 21, 28, 35, 42 and 49. Then, after oxidation, the most changes are restricted for these sites and their neighboring atoms which exhibit a more higher atomic charge. In the other hand, the resulting spin density distribution (fig.13-c), demonstrates also for doped PANI, only nitrogen atoms exhibits higher spin density. These first preliminary results let to conclude that the reactive sites are located around the nitrogen atoms.

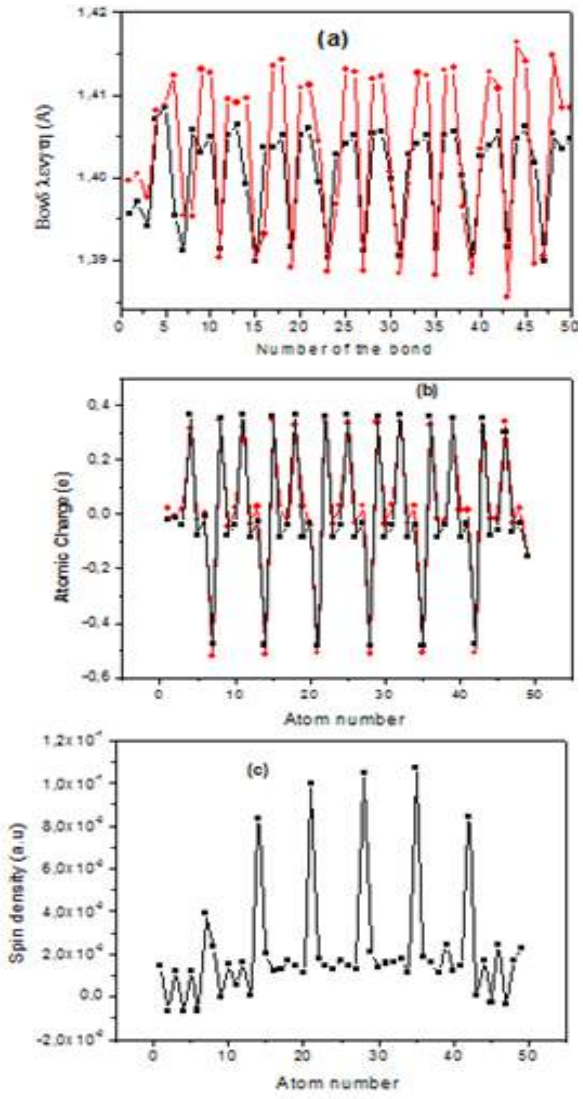

Fig 13. Changes of bond length (a), of atomic charge (b) from doped (■) to the it's oxidized state (●) and the resulting spin density at the doped state (c).

As, it is shown, changes of vibrational frequencies are limited around the nitrogen atoms in the polymer squeleton. These results are in good agreement with the observed changes in atomic charges and in the geometric parameters. Therefore, the most probable site of interaction for which carbon nanotubes can be grafted is the nitrogen atoms. This result was already supported by a systematic SERS and

FTIR experimental study on the neutral PANI/SWCNTs composite (Baibarac et al*.*, 2003). As it is known, carbon nanotubes have unique electronic properties (Chenand Yu*,* 2005) and the already proposed grafting mechanism are checked by electronic changes involving C=C groups which constitutes the tube (Zaidi et al*.*, 2010). Our modeling structure of the nano-composite is based on the covalent bonding between both components (fig.14). It is of importance to note that, the non-covalent bonding can be also present on the final structure. These non-covalent bonding are due to the intensive Van der Walls cohesive Force for carbon nanotubes which inhibit the homogenous dispersions process (Byron et al*.*, 20; Schroder et al*.*, 2003).

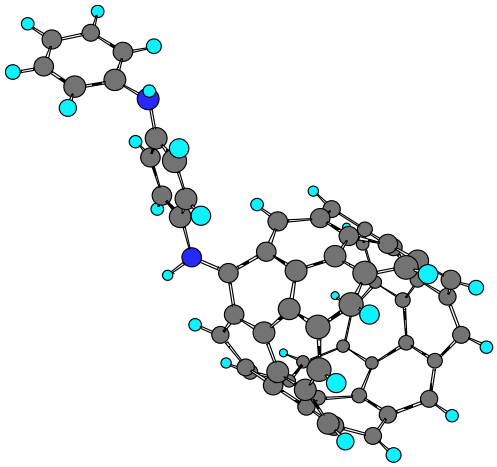

Fig 14. Modeling structure of the nano-composite D-PAN/SWCNTs.

To support this hypothesis, fig.15 represents the change of optical absorption spectra after doping and after SWCNTs adding obtained either experimentally or theoretically. From this figure, same transitions are found and a decrease of the optical gap after doping and after SWCNTS adding is clearly seen in both cases which support the already proposed grafting mechanism.

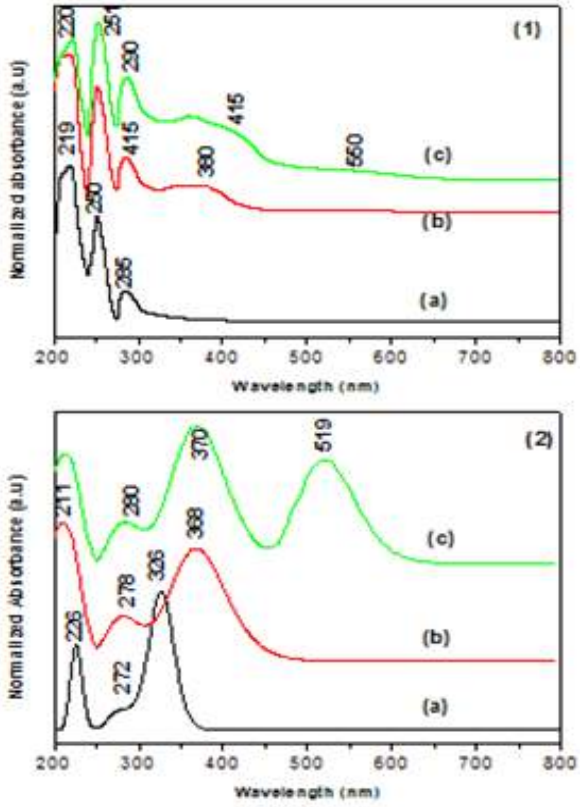

Fig.15. (1) Experimental (1) and theoretical (2) optical absorption spectra (a) PANIEB, (b) of sulfonic acid doped PANI and of the nano-composite (c).

From experimental to theatrical spectra, it is noted that band intensities of theoretical spectra are more pronounced. This difference is principally due to the fact that calculations are done on the modeling structure already presented in fig. 14, for which the SWCNTs concentration is higher than that used in experimental part. Moreover, experimentally, the doping process is accomplished via adding acid entities which lead to the molecular structure modification. Theoretically the process is accomplished only by electron adding. As it is demonstrated for PANI at its

neutral state, the π-π* transition which dominates the energy gap is maximized at 290 nm and the corresponding energy gap is 3.75 eV. The other transitions at higher energy (lower wavelength) are however attributed to σ- σ* and σ- π* transitions (Farag et al*.*, 2010).

For the doped polyaniline, a large band is created giving rise to the optical gap decrease. This gap reduction is due to the π-polaron and/or polaron-π* band transitions (Huangand MacDiarmid, 1993). This new band results on the decrease of the optical gap at the onset of nearly 2.63 eV. When SWCNTs are added, the spectrum is dramatically changed and a new band appears at λ_{max} = 535 nm, giving rise the onset of optical absorption at nearly 1.7 eV. As it is already reported, this new band is attributed to the charge transfer (Zaidi et al*.*, 2011). In fact, photo-excitation begins in the polymer matrix and after electron diffusion; electron can be easily transferred to the SWCNTs as it reported for some polymer/SWCNTs nano-composites (Jeong et al*.*, 2015). This charge transfer is the major parameter for which the improvement of photovoltaic characteristics is referred (He et al*.*, 2014).

By referring to the experimental spectra, theoretically, optical absorption spectra relative to the neutral, doped or functionalized with SWCNTs states show also that same transitions are found, except a shifting. The observed shifting is probably due to the fact that calculations are done in gaseous phase and without inter-chain interaction. The above presented experimental results and the obtained theoretical calculations supports the modeling structure and consequently the grafting process which take place in the nitrogen atom.

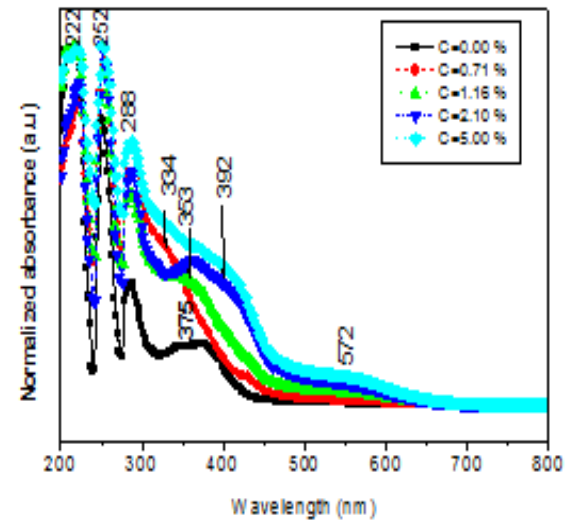

Fig 16. Variation of optical absorption spectra of doped PANI/SWCNTs composite versus the SWCNTs

In other hand and in order to evaluate the most appropriate SWCNTs weight concentration, which permits to evaluate the most appropriate photovoltaic characteristics, fig.16 represents the evolution of optical absorption spectra as a function of SWCNTs contents. First, it is clearly seen that sulfonic acid doping induces the creation of new additional band centered at λ_{max} =340 nm which show a progressive broadness. This latter is progressively red - shifted as a function of SWCNTs weight concentrations to be centered at 392 nm for both higher SWCNTs weight concentrations (2.16 % and 5.0 %). Moreover, localized states due to the charge transfer creation within the energy gap are clearly seen after SWCNTs functionnalization (Goswami et al*.*, 2016), as shown, by the appearing of new additional feature in the wavelength ranging from 500 to 650 nm. In order to evaluate the effect of either acid doping or SWCNTs adding on the electronic structure of the basic material, the evolution of the optical energy gap and those of localized state the most significant parameters.

The band gap all compounds presented in this study has been estimated from the absorbance coefficient data as a function of wavelength using Tauc relation as given by equation 1 (Eq. 8) (Tauc, 1974). Where α is the absorption coefficient, hυ is the photon energy, B is the band gap tailing parameter, Eg is the optical band gap and n is the transition probability index. By the plot of $(\alpha h\boldsymbol{\nu})^{1/2}$ versus h$\boldsymbol{\nu}$ (fig. 17-1), the energy gap is estimated by extrapolation of the linear dependence which occurs generally in the absorption onset (Chithralekha et al., 2007; Kumar, 2011). From fig. 16, it is also noted that when SWCNTs are added a new feature appears in wavelength ranging from 500 to 650 nm. This new band which is progressively more pronounced when SWCNTs increase traduces the creation of localized states within the energy gap. In fact in the low photon energy range, the spectral dependence of the absorption coefficient (α) and photon energy (hv) is known as Urbach empirical rule, which is given by the following equation (Eq. 9) (Urbach, 1953):

$$\alpha h\nu = B(h\nu - Eg)^n \qquad \text{(Eq. 8)}$$

$$\alpha = \alpha_0 \exp\left(\frac{h\nu}{E_U}\right) \qquad \text{(Eq. 9)}$$

where α_0 is a constant and EU denotes the energy of the band tail or sometimes called Urbach energy (Kumar, 2011), which is weakly dependent upon temperature and is often interpreted as the width of the band tail due to localized states in the normally band gap that is associated with the disordered or low crystalline materials (Urbach et al., 1953; Kazmersky et al., 1985). Taking the logarithm of the two sides of Eq. 9, hence one can get a straight line equation (Eq. 10). Therefore, the band tail energy or Urbach energy (EU) can be obtained from the slope of the straight line of plotting ln (α) against the incident photon energy (hα) (Fig.17-2).

$$\mathrm{Ln}\,(\alpha) = \mathrm{Ln}\,(\alpha_0) + \frac{h\nu}{E_U} \qquad \text{(Eq. 10)}$$

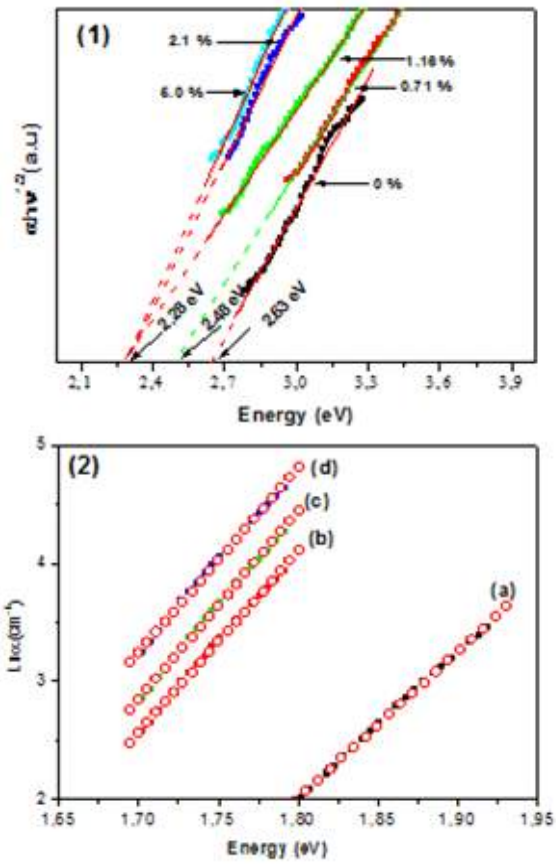

Fig 17. (1): Variation of $(\alpha h\boldsymbol{\nu})^{1/2}$ versus hv in the onset of absorbance region, (2): Evaluation of band tail width of localized states as a function of SWCNTs weight concentrations: (a) 0.71 %, (b): 1.16 %, (c): 2.1% and (d): 5%.

All the data concerning the optical gap and the localized states are summarized in fig.17. The obtained energies gap for doped polyaniline is 2.63 eV. Then, when adding

SWCNTs, this later takes the values of 2.48 eV for the lower SWCNTs concentrations and is typically the same (2.28 eV) for the other SWCNTs concentrations. The evolution of the optical gap as a function of SWCNTs concentrations presented on the onset of fig.17 demonstrates that it has a limit of 2.28 eV whatever are the SWCNTs concentrations. For the lower SWCNTs concentration (0.71), the new localized state which traduces the charge transfer creation has threshold energy of 1.7 eV. Starting from the 1.16% Weight concentration the SWCNTs weight increase has no significant effect on the energy position of localized states. Indeed, for all concentrations higher than 0.71 wt %, this threshold energy is typically 1.62 eV. The band width of localized states takes respectively 80 meV for the first SWCNTs concentration and nearly 65 meV for the other SWCNTs Concentrations. The challenge is now to check the properties of this charge transfer availability between both components and to carry out the electronic properties of the resulting nano-composite (Zaidi et al., 2011). The obtained electronic structure permits to elucidate the aptitude of the doped polyaniline on the photovoltaic conversion when the structure is regularly dispersed with SWCNTs to avoid an interpenetrating network. Principally, some electronic parameters such as HOMO, LUMO levels and ionization potential energy should be known. For these reasons and in order to evaluate the electronic structure of the used compounds, fig. 18 represents the evolution of the HOMO-LUMO energies levels of both neutral and doped states for several units cells. Same procedure has been previously used in order to elucidate electronic affinity and ionization potential for infinite chain length (Aleman et al., 2008).

As it is represented, these energetic levels show a linear relation-ship as a function of 1/n. The extrapolation for infinite chains (1/n→0) permits to elucidate the corresponding electronic energy gap which is evaluate to be 3.58 eV for polyaniline and 2.31 eV for the doped polyaniline. These values are in accordance with the already published experimental results (Aleman et al., 2008). The decrease of the electronic gap is evidently due to the creation of new energetic levels on the band gap of the neutral polymer as it is reported in the experimental part. In fact, for the doped polyaniline, the obtained energy value is lower than that obtained experimentally by nearly 0.5 eV. This difference can be related to the chain length diminution after sulfonic acid doping and to the weak inter-chain interaction due to the solvent state.

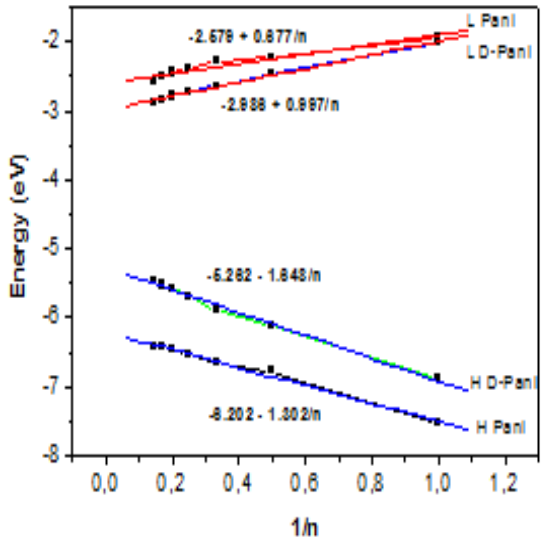

Fig 18. The evolution of the HOMO-LUMO energies levels of both neutral and doped states for several units cells (n).

To more support this hypothesis concerning the charge transfer and the ability of electron or hole transport, fig. 19 shows the contour plots

of molecular orbital (MOs) including HOMO and LUMO of both compounds. The HOMO possessed an anti-bonding p character between the two adjacent subunits (Mayand Kühn*.,* 2011). However, the LUMO has a bonding character between the two subunits. When passing from ground to excited states, the HOMO state density was much localized on the donor moiety, while the electron density of LUMO was mainly localized on the acceptor moiety (El Malki et al*.,* 2016).

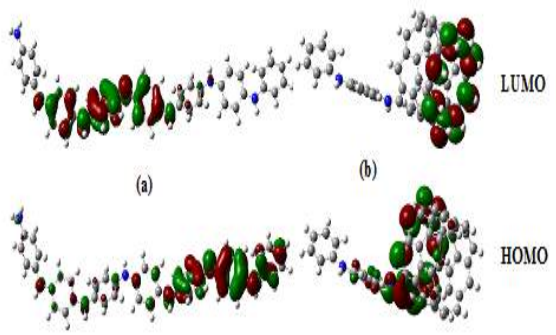

Fig 19. The contour plots of HOMO and LUMO orbitals of the studied compounds in their ground states: (a) doped polyaniline, (b) the nano-composite D-PANI/SWCNTs.

To evaluate the aptitude of the resulting interpenetrating network, on the photovoltaic conversion, some parameters should be cheeked such as the open-circuit voltage Voc and the power conversion efficiency (PCE). These parameters are related by (Eq. 11) (Mabrouk et al*.,* 2013), where Pin is the incident power density and FF is the Field factor.

$$PCE = \frac{FF.V_{OC}.\ Isc}{P_{in}} \qquad \text{(Eq. 11)}$$

The power conversion efficiency can also be checked theoretically from the Scharber diagram. This parameter is strictly related to the electronic structure of both components. In the other hand, as it is previously described (Gadisa et al*.,* 2004), it is possible to evaluate the open-circuit voltage Voc theoretically from the difference between HOMO and LUMO Energies levels of respectively donor and acceptor materials (Eq. 12).

$$V_{OC}(V) = \frac{1}{e}\left|E(HOMO)^{donor}(eV)\right| - \left|E(LUMO)^{acceptor}(eV)\right| - 0.3\ (V)$$

(Eq. 12)

Here e is the elementary charge and 0.3 V is a typical loss found in bulk hetero-junction solar cells due energy lost during the photo-charges generation (Azazi et al*.,* 2011). A similar relation has been reported by Veldman et al., and Scharber et al., (Veldman et al*.,* 2009; Scharber et al*.,*2013). For the SWCNTs alone, same calculations are also done on its modeling structure. Results give that SWCNTs exhibits HOMO and LUMO energy level respectively of 5.3 eV and 3.7 eV, by referring to vacuum level. These results are in good agreement with those recently reported (Ferguson et al*.,* 2013). By comparing the obtained energetic levels for both doped polyaniline and SWCNTs to those of the work function of some metals, ITO and Al are the most appropriate for the architecture of the resulting solar cell (fig.20-a). From this electronic structure, the open circuit voltage (Voc) is nearly 1.25 V.

As it is presented above in, localized states have the threshold energy of 1.62 eV. This energy coincides with those between HOMO of doped polyaniline and LUMO of SWCNTs energy levels. In fact, at this nanometer scale the transfer under illumination of electron between these energy levels is possible; especially for this interpenetrating network when the

diffusion length is typically the same of chain length. Indeed, photo-excitation begins in the polymer matrix and finishes on the SWCNTs squeleton. Then, starting from the energy diagram of the resulting photovoltaic cell presented in fig.20-a, it is possible to estimate the maximum power conversion efficiency which is strictly based on from Scharber diagram (fig.20-b).

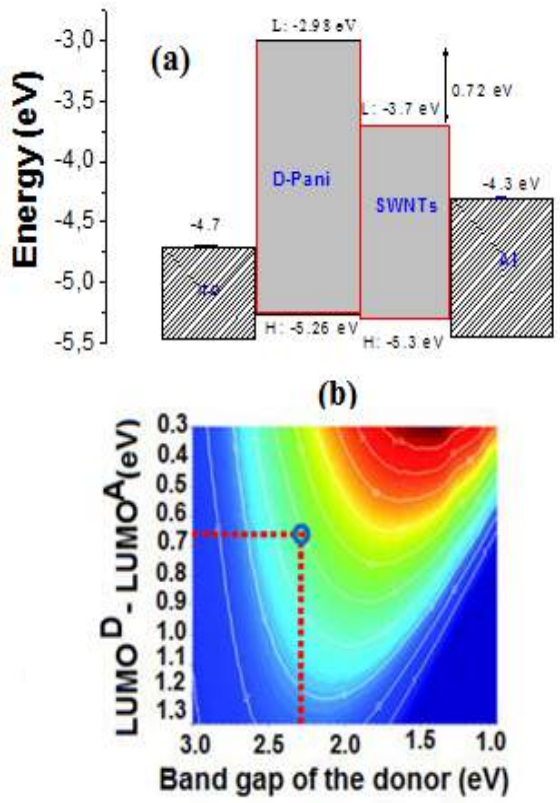

Fig 20. (a) Energetic diagram of the bulk hetero-junction ITO/Doped PANI/SWCNTs/Al photovoltaic cell (b) the power conversion efficiencies. D: Donor, A: Acceptor (Azazi, 2011; Veldman, 2009).

The resulting interpenetrating network exhibits a power conversion efficiencies (PCEs) varying from the 4% to 5%. Note that the power conversion efficiency can be ameliorated by using short-oligo aniline rather than the polymer. However, the chain length (number of units) should be chosen as a function of its compatibility with the solar spectrum in the absorption process and as a function of the electron diffusion length (Zaidi et al*.,* 2013).

9. Conclusions

Intensive efforts have been devoted in the two last decades in order to obtain organic nano-composites with advanced functional properties, incorporating well-dispersed and aligned CNTs. However, majority of these experimental methods are not able to produce CNTs/polymer nano-composites with properties comparable to those theoretically provided. The possibility of synthesizing advanced nano-composites with perfectly aligned CNTs is still uncertain and depends on the properties, the perfection and the dispersion quality of CNTs structure. In the other hand its necessary to overcame Van der Waals forces and to control polymer/CNTs interfaces. Our interested is focused on synthestising polyaniline/ SWCNTs nano-composite. For that, Polyaniline EB is treated with sulfonic acid, and functionalized with SWCNTs. A systematic experimental study based on change of vibration and optical properties is established as a function of SWCNTs contents. In the other hand, and by referring to the experimental conclusions, a theoretical study based on DFT calculations is also done in order to establish correlation structure-properties. Results show that a covalent bonding between doped polyaniline and SWCNTs is occurred via nitrogen link. This functionalization process induces the appearing of new broad band giving rise to a decrease of optical gap to reach the value of 2.28. The obtained nano-composite exhibits a good compatibility with the solar spectrum.

Moreover, whatever the SWCNTs weight concentrations, a localized state within the gap having the threshold energy of 1.62 eV is created. This localized state is the consequence of the donor-acceptor charge transfer. The modeling of the bulk hetero-junction photovoltaic cell ITO/D-PAN/SWCNTs/Al is also elucidated. The open voltage circuit is evaluated nearly 1.25 V and the corresponding power conversion efficiencies (PCEs) is estimated to be 4~ 5 %.

References

Ahllskog, M., Menon. R., Heeger. A. J., Noguchi. T. and Ohnishi. T. (1997). Metal-insulator transition in oriented poly(p-phenylenevinylene). *Physical Review B*. 55: 6777-6787.

Aleman, C., Ferreir, C. A., Torras, J., Meneguzzi, A., Canales, M., Rodrigues, M. A.S, Casanovas, J. (2008).On the molecular properties of polyaniline: A comprehensive theoretical study.*Polymer*. 49: 5169- 5176.

Alimi, K., Zaidi, B. and Chemek, M. (2011), About Grafting of Single-walled Carbon Nanotubes on the Oligo-N-vinyl Carbazole and Copolymer Involving N-vinylcarbazole and Hexylthiophene, Book chapter, Intch Open access, *Carbon Nanotubes – Polymer Nanocomposites*. Pp. 300-330.

Arnold, M. S., Green, A. A., Hulvat, J. F., Stupp, S. I., and Hersam, M. C. (2006). Sorting carbon nanotubes by electronic structure using density differentiation. *Nature Nanotechnology*. 1: 60-65.

Arnold, M. S., Stupp, S. I., Hersam, M. C. (2005). Enrichment of single-walled carbon nanotubes by diameter. *Nano Lett*er. 5: 713-718.

Ayachi, S., Alimi, K., Bouachrine, M., Hamidi, M., Mevellec, J. Y. and Porte, J. P. L. (2006). Spectroscopic investigations of copolymers incorporating various thiophene and phenylene monomers. *Synthetic Metals.* 156: 318.

Ayachi, S., Ghomrasni, S. and Alimi, K. (2012). A combined experimental and theoretical study on vibrational and optical properties of copolymer incorporation g thienylene-dioctyloxyphenylene and bipyridine units. *J. Applied Polymer Science.* 123: 2684.

Azazi A., Mabrouk A., Alimi, K. (2011). Theoretical investigation on the photophysical properties of low-band-gap copolymers for photovoltaic devices. *Computational Theoretical Chemistry.* 978: 7-15.

Baibarac, M., Baltog, I., Lefrant, S., Mevellec, J.Y., Chauvet, O. (2003). Polyaniline and Carbon Nanotubes Based Composites Containing Whole Units and Fragments of Nanotubes. *Chemica Materials.* 15: 4149-4156.

Becke, A. D. (1993). Density functional thermochemistry. III. The role of exact exchange .*J. Cheical Phyisics*. 98: 5648.

Bejbouji, H., Vignau, L., Miane, J. L., Dang, M. T., ElMostafa, O., Harmouchi, M., Mouhsen, A. (2010). Polyaniline as a hole injection layer on organic photovoltaic cells, Solar Energy Materials and Solar Cells. *Solar Energy and Mateials Solat Cells*. 94: 176-181.

Boncel, S., Koziol, K. K. K. , Walczak, K. Z., Windle, A. H. , Shaffer, M. S. P. (2011). Infiltration of highly aligned carbon nanotube arrays with molten polystyrene. *Materials Lett*er. 65: 2229-2303.

Bonard, J. M. , Stora, T., Salvetat, J. P., Maier, F., Stockli, T. and Dusch, C. 1997). Purification and size selection of carbon nanotubes. *Advanced. Materials*. 9: 827-831.

Bourass, M., Benjelloun, A. T., Benzakour, M., Mcharfi, M., Hamidi, M., Bouzzine, S. M.,

Serein-Spirau, F., Jarrosson, T., Lère-Porte, J. P., Sotiropoulos, J. M. and Bouachrine, M. (2016). The Computational Study of The electronic and Optoelectronics Properties of New Materials Based On Thienopyrazine For Application in Dye Solar Cells. *Journal materials and Environmental Science.* 7: 700-712.

Bronikowski, M. J., Willis, P. A., Colbert, D. T., Smith, K. A., and Smalley, R. E. (2001). Gas-phase production of carbon single-walled nanotubes from carbon monoxide via the hipco process: A parametric study. *Journal of vacuum Science & technology A-Vacuum surfaces and films*. 19: 1800-1805.

Burroughes, J. H., Bradley, D. D. C., R. Brown, A., Maorks, R. N., Mackey, K., Friend, R. H., Burn, P. L. and Holmes, A. B. (1990). Electroluminescence on conjugated polymer. *Nature. pp.* 547- 569.

Byron, P. R., Hubert, P., Salvetat, J. P. and Zalamea, L. (2006). Flexural deflection as a measure of van der Waals interaction forces in the CNT array. *Composite Science and Technology.* 66: 1125-1131.

Cao, Y., Smith, P. and Heeger, A. J. (1989). Spectroscopic studies of polyaniline in solution and in spin-cast films .*Synthetic Metals.* 32: 263-281.

Cao, Y. (1990). Spectroscopic studies of acceptor and donor doping of polyaniline in the emeraldine base and pernigraniline forms. *Synthetic Metals.* 35: 319-332.

Carter, J. C, Grizzi, I., Heeks, S. K., Lacey, D. J., Latham, S. G., May, P. G., Ruiz, O., Pickler, K., Towns, C. R. and Wittman, H. F. (1997). Operating stability of light-emitting polymer diodes, based on poly (p-phenylenevinylene). *Applied Physics Lett*er. 71: 34-36.

Chakrabarti, S., Das, B., Banergi, P., Bnerjee, B. and Bhattacharya, R. (1999). Bipolaron saturation in polyperrole. *Physical Review B*. 60 (11): 7691-7694.

Chaudhuri, D., Kumar, A., Rudra, I. and Sarma, D. D. (2001). Synthesis and SpectroscopicCharacterization of Highly Conducting BF3-Doped Polyaniline. *Advanced. Mateials*. 13: 1548-1551.

Chen, X. Q. , Saito, T. , Yamada, H. and Matsushige, K. (2001). Aligning singlewall carbon nanotubes with an alternating-current electric field . *Applied Physics Letter*. 78: 3714-3716.

Chen, G.X., Li, Y. and Shimizu, H. (2007). Ultrahigh-shear processing for the preparation of polymer/carbon nanotube composites. *Carbon*. 45: 2334-2340.

Chen, Y. and Yu, J. (2005). Growth direction control of aligned carbon nanotubes. *Carbon*. 43:3181-3194.

Chiang, J. C. and MacDiarmid, A. G. (1986).Protonic acid doping of the emeraldine form to the metallic regime. *Synthetic Met*als. 13: 193-205.

Chithralekha, P., Subramanian, and Padiyan, D. P. (2007). Electrodeposition of polyaniline thin films doped with dodeca tungstophosphoric acid: Effect on annealing and vapor sensing. *Sensors and Actuators B: Chemical.* 122: 274-281.

Choi, E. S., Brooks, J.S., Eaton, D. L., Al-Haik, M. S., Hussaini, M. Y., Garmestani, H., Li, D. and Dahmen, K. (2003). Enhancement of thermal and electrical properties of carbon nanotube polymer composites by magnetic field processing. *J. Applied Physiol*ogy. 94: 6034-6039.

Cholli, A. L., Thiyagarajan, M., Kumar, J. and Parmar, V. S. (2005). Biocatalytic approaches for synthesis of conducting polyaniline nanoparticles . *Pure Applied Chemistry.* 77 (1): 339-344.

Colanei, N., Nowak, M., Spiegel, D., Hotta, S. and Heeger, A. (1987). Bipolarons in poly (3-methylthiophene): spectroscopic, magnetic and electrochemical measurements. *Phyical Review B*. 36(15): 7964- 7968.

Cosnier, S. and Holzinger, M. (2008). Design of carbon nanotube-polymer frameworks by electropolymerization of SWCNT-pyrrole derivatives.*Electrochimica Acta.* 53(11): 3948-3954.

Deng, J., Ding, X., Zhang, W., Peng, Y., Wang, J., Long, X., Li, P. and Chan, A. (2002). Carbon nanotube– polyaniline hybrid materials . *European Polymer Jouranl*. 38: 2497-2501.

Deng, P., Lei, Y., Zheng, X., Li, S., Wu, J., Zhu, F., Ong, B. S. and Zhang, Q. (2016). Polymer based on benzothiadiazole-bridged bis-isoindigo for organic field-effect transistor applications. *Dyes and Pigm*ents. 125: 407-413.

Derbal-Habak, H., Bergeret, C., Cousseau, J. and Nunz, J. M. (2011). Improving the current density Jsc of organic solar cells P3HT: PCBM by structuring the photoactive layer with functionalized SWCNTs.*Solar Energy Materials & Solar. Cell*s. 95: 553-556.

DiCesare, N., Belletete, M., Marrano, C., Leclerc, M. and Durocher, G. (1998). Conformational Analysis (ab initio HF/3-21G*) and Optical Properties of Symmetrically Disubstituted Terthiophenes *J. Physical Cheme. A* 102: 5142-5149.

Dimaki, M. and Bøggild, P. (2004). Dielectrophoresis of carbon nanotubes using microelectrodes: a numerical study. *Nanotechnology.* 15: 1095-1102..

Dimitriev, O. P. (2004). Doping of polyaniline by transition metal salts: effect of metal cation on the film morphology. *Synthetic Metals*. 142: 299-303.

Domingues, D., Logakis, E. and Skordos, A. A. (2012). The use of an electric field in the preparation of glass fibre/epoxy composites containing carbon nanotubes .*Carbon*. 50: 2493-2503.

Ebbesen, T. W. (1994). Carbon nanotubes. *Annual review of materials science.* 24: 235–264.

El Malki, Z., Bouzzine, S. M., Bejjit, L., Haddad, M., Hamidi, M. and Bouachrine, M. (2011). Density functional theory [B3LYP/6-311G(d, p)] study of a new copolymer based on carbazole and (3,4-ethylenedioxythiophene) in their aromatic and polaronic states .*J. Applied Polymer Science.* 122: 3351-3360.

El Malki, Z., Bouachrine, M., Hamidi, M., Serein-Spirau,F., Lere-Porte, J. P. and Sotiropoulos, J. M. (2016). Theoretical study of New Donor-π-Acceptor compounds based on Carbazole, Thiophene and Benzothiadiazole for Photovoltaic application as Dye-sensitized solar cells. *Journal Materials and Environnemental Science.* 7 (9):3244-3255.

Farag, A. A. M., Ashery, A.and AbdelRafea, M. (2010): Optical dispersion and electronic transition characterizations of spin coated polyaniline thin films. *Synthetic Metals.*160: 156-161.

Ferguson, A. J., Blackburn, J. L. and Kopidaki, N. (2013). Fullerene and carbon nanotubes as acceptor materials in organic photovoltaic. *Materials Lett*er. 90: 115-125.

Franck, S., Poncharal, P., Wang, Z. L., and de Heer, W. A. (1998). Carbon nanotube quantum resistors. *Science.* 280: 1744-1746.

Freitag, M., Perebeinos, V., Chen, J., Stein, A., Tsang, J. C., Misewich, J. A., Martel, R. and Avouris, P. (2004). Hot carrier

electroluminescence from a single carbon nanotube. *Nano Letters*. 4: 1063–1066.

Frisch, M. J., Trucks, G.W., Schlegel, H. B., Scuseria, G. E., Robb, M. A. and Cheeseman, J. R. (2009*). Gaussian 09*, revision B.01. Wallingford CT: *Gaussian*, Inc.

Futaba, D. N., Mizuno, K., Namai, T., Yumura, M. and Iijima. S. (2004). Water-assisted highly efficient synthesis of impurity-free single-walled carbon nanotubes. *Science.* 306: 1362– 1364.

Gadisa, A., Svensson, M., Andersson, M. R. and Inganas, O. (2004). Correlation between oxidation potential and open-circuit voltage of composite solar cells based on blends of polythiophenesÕ fullerene derivative. *Applied Physics Letter.* 84: 1609-1611.

Gao, G. Yu, J., Hummelen, J. C., Wudl, F. and Heeger, A. J. (1995). Polymer Photovoltaic Cells: Enhanced Efficiencies via a Network of Internal Donor-Acceptor Heterojunctions *Science*. 270: 1789-1791.

Genoud, F., Kulszewicz-Bajer, I., Bedel, A., Oddou, J. L., Jeandey, C. and Pron, A. (2000). Lewis Acid Doped Polyaniline. Part II: Spectroscopic Studies of Emeraldine Base and Emeraldine Hydrochloride Complexation with FeCl3. *Chemical Materials.* 12: 744.

Gohier, A., Minéa, T. M., Djouadi, M. A. and Granier, A. (2007). Impact of the etching gas on vertically oriented single wall and few walled carbon nanotubes by plasma enhanced chemical vapor deposition. *Journal of Applied Physics.*101: 054317-54322.

Gojny, F.H. , Nastalczyk, J., Roslaniec, Z. and Schulte, K. (2003). Surface modified multi-walled carbon nanotubes in CNT/epoxy-composites, *Chemical Physics Letters*. 370: 820-824.

Gorelsky, S. I. (2009). *Swizard Program*, University of Ottawa, Canada

Goswami, M., Ghosh, R., Maruyama, T. and Meikap, A. K. (2016). Polyaniline/carbon nanotube/CdS quantum dot composites with enhanced optical and electrical properties. *Applied Surface Science.* 364: 176-180.

Guo, T., Nikolaev, P., Thess, A., Colbert, D. T. and Smalley, R. E. (1995). Catalytic growth of single-walled nanotubes by laser vaporization. *Chemical physics letters*. 243: 49-54.

Han, Y. K., Chang, M. Y., Ho, K. S., Hsieh, T. H., Tsai, J. L. and Huang, P. C. (2014). Electrochemically deposited nano polyaniline films as hole transporting layers in organic solar cells. *Solar Energy Materials and Solar Cells.* 128: 198-203.

Harigay, K. (1992). Metal-insulator transition in doped conducting polymers. Disappearance of the electronic gap with persisting bond alternation in the system with site-type impurities. *Chemical Physics.* 167: 315-326.

He B., Tang, Q., Luo, J., Li, Q., Chen X. and Cai, H. J. (2014). Rapid charge-transfer in polypyrrole–single wall carbon nanotube complex counter electrodes: Improved photovoltaic performances of dye-sensitized solar cells.*Power Sources*. 256: 170-177.

Heeger, A. J. (2001). Nobel Prize 2000 lecture: Semiconducting and metallic polymers: The fourth generation of polymeric materials*. Current Applied Physics*. 1: 247-267.

Hone, J. (1999). Thermal conductivity of single-wall carbon nanotubes. *Synthetic metals*. 103: 2498-2499.

Hone, J., Llaguno, M.C., Nemes, N. M., Johnson, A. T., Fischer, J. E., Walters, D. A. (2000). Electrical and thermal transport properties of magnetically aligned single wall carbon nanotube films. *Aplied Physics. Lettter*. 77: 666-668.

Hongwei, W. Zhu, J., Wang, K. and Wu, D. S. (2009).Applications of carbon materials in photovoltaic solar cells. Solar Energy Materials and Solar Cells. *Cells*. 93:1461-1470.

Holzinger, M., Steinmetz, J., Samaille, D., Glerup, M., Paillet, M., Bernier, P., Ley, L. and Graupner, R. (2004). Cycloaddition for cross-linking SWCNTs. *Carbon*. 42: 941-947.

Hu, H., Yu, A., Kim, E., Zhao, B., Itkis, M. E. and Bekyarova, E. (2005). Influence of the Zeta Potential on the Dispersability and Purification of Single-Walled Carbon Nanotubes. *The Journal of Physical Chemistry B.* 109: 11520-11524.

Huang, W. S. and MacDiarmid, A. G. (1993). Optical properties of polyaniline.*Polymer.* 34: 1833-1845.

Huang, Y. Y. and Terentjev, E. M. (2012). Dispersion of Carbon Nanotubes: Mixing, Sonication Stabilization, and Composite Properties, Polymers. *Polym*er. 4: 275-295.

Hundley, M. F., Adams, P. N., Mattes, B. R. (2002). The influence of 2-acrylamido-2-methyl-1-propanesulfonic acid (AMPSA) additive concentration and stretch orientation on electronic transport in AMPSA-modified polyaniline films prepared from an acid solvent mixture. *Synthetic Meals.* 129: 291-297.

IIjima, S. (1991). Helical microtubules of graphitic carbon. *Nature.* 354: 56-58.

Iijima, S. and Ichihashi, T. (1993). Single-shell carbon nanotubes of 1-nm diameter . *Nature*. 363: 603-605.

Janssen, R. A. J., Hummelen, J. C., Sariciftci, N. S. (2005). Polymer–Fullerene Bulk Heterojunction Solar Cells. *MRS Bull*etin. 30: 33-36.

Jeong, D. C., Song, S. G., Satheesh, Kumar, C., Lee, Y., Kim, K. S. and Song, C. (2015). Enhanced photo-induced electron transfer by multi-walled carbon nanotubes in self-assembled terpyridine polymer networks.*Polym*er. 69: 39 - 44.

Journet, C., Maser, W. K., Bernier, P., Loiseau, A., Lamy C. M., Lefrant, S., Deniard, P., Lee, R. and Fischer, J. E. (1997). Large-scale production of single-walled carbon nanotubes by the electric-arc technique. *Nature*. 388: 756-358.

Jun, G. H., Jin, S. H., Park, S. H., Jeon, S. and Hong, S. H. (2012). Highly dispersed carbon nanotubes in organic media for polymer: fullerene photovoltaic devices.*Carbon*. 50: 40-46.

Kazmersky, L. L. (1980). Polycrystalline and Amorphous Thin Films and Devices, *Academic Press*, New York. pp.135.

Kerr, C. J., Huang, Y. Y., Marshall, J. E. and Terentjev, E. M. (2011). Effect of filament aspect ratio on the dielectric response of multi-walled carbon nanotube composites. *Journal Applied Physics*. 109: 094109-094109-6.

Khoshkholgh, M. J., Marsusi, F. and Abolhassani, M. R. (2015). Abolhassani, Density functional theory investigation of opto-electronic properties of thieno [3,4-b] thiophene and benzodithiophenepolymer and derivatives and their applications in solar cell. *Spectrochimica Acta Part A*. 136: 373-380.

Kitiyanan, B., Alvarez, W. E., Harwell, J. H. and Resasco, D. E. (2000). Controlled production of single wall carbon nanotubes by catalytic decomposition of co on bimetallic como catalysts. *Chemical Physics Letter*. 317: 497-503.

Kim, K. and Jin, J. I. (2001). Preparation of ppv nanotubes and nanorods and carbonized products derived therefrom. *Nano letters.* 1(11): 631-636.

Kong, J., Yenilmez, E., Tombler, T. W., Kim, W. and Dai, H. (2001). Quantum interference and ballistic transmission in nanotube electron waveguides. *Physical review letters.* 87: 106801-106807

Kong, J. and Dai, H. (2001). Full and Modulated Chemical Gating of Individual Carbon Nanotubes by Organic Amine Compounds. *The journal of physical chemistry B*. 105: 2890-2893.

Kovac, J., Peternai, L. and Lengyel, O. (2003). Advanced light emitting diodes structures for optoelectronic applications. *Thin Solids Films*. 433: 22-26.

Krupke, R., Hennrich, F., Lohneysen, H. V. and Kappes, M.M. (2003). Separation of Metallic from Semiconducting Single-Walled Carbon Nanotubes. *Science*. 301: 344-347.

Kulszewicz-Bajer, I., Pron, A., Abramowicz, J., Jeandey, C., Oddou, J. L. and Sobczak, J. W. (1999). Lewis Acid Doped Polyaniline: Preparation and Spectroscopic Characterization. *Chemical Materials*. 11(3): 552-556.

Kumar, A. (2011). Swift heavy ion irradiation induced modifications in the optical band gap and Urbach's tail in polyaniline nanofibers. *Nuclear Instruments and Methods in Physics Research Section B*. 269: 2798-2806.

Lee, C., Yang, W. and Parr, R. G. (1988). Development of colle-salvetti correlation energy formula, into a functional of the electron density. *Physical Review B.* 37: 785-789.

Lee, R. S., Kim, H. J., Fischer, J. E., Thess, A. and Smalley, R. E. (1997). Conductivity enhancement in single-walled carbon nanotube bundles doped with k and br. *Nature*. 388: 255-257.

Lee, C. H., Lee, C. E. and jin, J. I. (1998). Bipolaron formation on I2-doped PBMPV conducting polymers. *J. of the Korean Society*. 33: 532-534.

Liu, J.Q., Xiao, T., Liao, K. and Wu, P. (2012). Interfacial design of carbon nanotube polymer composites: a hybrid system of noncovalent and covalent functionnalizations. *Nanotechnology.* 18: 165701.

Lizin, S., Passel, S. V., Schepper, E. D. and Vranken, L. (2012). The future of organic photovoltaic solar cells as a direct power source for consumer electronics. *Solar Energy Materials Solar Cells*. 103:1-10.

Lu, S. and Panchapakesan, B. (2006). Photoconductivity in single wall carbon nanotube sheets. *Nanotechnology.* 17: 1843-1850.

Lu, X., Hu, Y., Wang, L., Guo, Q., Chen, S., Chen, Sh., Hou, H. and Song, Y. (2016). Macroporous Carbon/Nitrogen-doped Carbon Nanotubes/ Polyaniline Nanocomposites and Their Application in Supercapacitors. *Electrochimica Acta.* 189: 158-165.

Mabrouk, A., Azazi, A. and Alimi, K. (2013). Molecular structure–property engineering of low-band-gap copolymers, based on fluorene, for efficient bulk heterojunction solar cells: A density functional theory

study. *Polymer Engineering Science*. 53:1040-1052.

MacDiarmid, A. G. (1997). Polyaniline and polypyrrole: Where are we headed. *Synthetic Met*als. 84: 27-34.

Malinauskas, A. (2001). Chemical deposition of conducting polymers. *Polymer.* 42: 3957-3972.

Martin, R, Céspedes-Guirao, F. J., Miguel, M. D., Lazaro, F. F., García, H. and Sastre, S. (2012). A. Single and multi-walled carbon nanotubes covalently linked to Synthesis, characterization and photophysical properties. *Chemical Science*. 3: 470-475.

May, V. and Kuhn, O. (2011). Charge and Energy Transfer Dynamics in Molecular Systems, 3rd Revised and Enlarged, *Edition Wiley, VCH*, *Berlin.* ISBN: 978-3-527-40732-3.

Mbarek, M., Zaidi, B., Wéry, J. and Alimi, K. (2012). Structure–properties correlation of copolymers derived from poly (phenylene vinylene) (PPV). *Synthetic Metals*. 162: 1762-1768.

Meyyappan, M., Delzeit, L., Cassell, A. and Hash, D. (2003). Carbon nanotube growth by PECVD: a review. *Plasma Sources Science and Technology*. 12: 205.

Mickelson, E. T., Huffman, C. B., Rinzler, A. G., Smalley, R. E., Hauge, R. H. and Margrave, J. L. (1998). Fluorination of Single-Wall Carbon Nanotubes. *Chemical Physics Letter.* 296: 188-194.

Mishra, A. K. and Tandon, P. (2009). Ab Initio and DFT Study of Polyaniline Leucoemeraldine Base and Its Oligomers *Journal Physical Chemistry B.* 113: 14629-14639.

Moaseri, E., Karimi M., Baniadam, M. and Maghreb, M. (2014). Improvements in mechanical properties of multi-walled carbon nanotube-reinforced epoxy composites through novel magnetic-assisted method for alignment of carbon nanotubes. *Composites Part A Applied Science and Manufacturing*: 64: 228-233.

Molapo, K. M., Ndangili, P. M., Ajayi, R. F., Mbambisa, G., Mailu, S. M., Njomo, N., Masikini, M., Baker, P. and Iwuoha, E. I. (2012).Electronics of Conjugated Polymers (I): Polyaniline. *International Journal Electrochemical Science.* 11859-11875.

Monti, M., Natali, M., Torre, L. and Kenny, J. M. (2012). The alignment of single walled carbon nanotubes in an epoxy resin by applying a DC electric field. *Carbon*. 50: 2453-2464.

Moradi, O., Yari, M., Zare, K., Mizra, B. and Najafi, F. (2012). A review of chemistry principles and reactions. *Fullerenes Nanotubes and Carbon Nanostructures*. 20: 138-151.

Morishita, T., Matsushita, M., Katagiri, Y. and Fukumori, K. (2010). Noncovalent functionalization of carbon nanotubes with maleimide polymers applicable to high-melting polymer-based composites. *Carbon*. 48: 2308-2316.

Mulligan, C. J., Bilen, C., Zhou, X. , Belcher, W. J.and Dastoor, P. C. (2015). Levelised cost of electricity for organic photovoltaics. *Solar Energy Materials and Solar Cells*.133: 26-31.

O'Connell, M. J., Bachilo, S. M., Huffman, C. B., Moore, V. C., Strano, M. S. and Haroz, E. H. (2002). Band gap fluorescence from individual single-walled carbon nanotubes. *Science*. 297: 593-596.

Pal, G., Kumar, S. (2016). Modeling of carbon nanotubes and carbon nanotube–polymer composites. *Progress in Aerospace Sciences*. 80: 33-58.

Park, C., Wilkinson, J., Banda, S., Ounaies, Z., Wise, K. and Sauti, G. (2006). Aligned

single-wall carbon Nanotubes polymer composite using an electric field. *Journal of Polymer Science part B*. 44: 1751-1762.

Park, S.D., Han, D.H., Teng, D. and Kwon, Y. (2008). Rheological properties and dispersion of multi-walled Carbon nanotube (MWCNT) in polystyrene matrix. *Current Applied Physics.* 8: 482-485.

Peng, H., Reverdy, P., Khabashesku, V. N. and Margrave, J. L. (2003). Side wall functionalization of single- walled carbon nanotubes with organic peroxides. *Chemical Communication*. 3: 362-365.

Peumans, P. and Forrest, S. R. (2001). Very-high-efficiency double-heterostructure copper phthalocyanine/C60 photovoltaic cells. *Applied Phyics Letter*. 79(1): 126-128.

Pickholz, M., dosSantos, M.C. (1999). Interchain and correlation effects in oligothiophenes. *Synthetic Metals.* 101: 528-529.

Pietro, W.J., Francl, M. M., Hehre, W. J., Defrees, D. J., Pople, J. A. and Binkley, J. S. (1982). Binkley, Self-consistent molecular orbital methods. 24. Supplemented small split-valence basis sets for second row elements. *Journal of American Chemical Society*. 104: 5039-5048.

Pinto, N.J., Johnson, A.T. J., MacDiarmid, A.G., Mueller, C. H., Theofylaktos, N., Robinson, D.C., Miranda, F.A. (2003). Electrospun polyaniline/polythethylene oxide nanofiber field-effect transistor. *Applied Physics Letter*. 83: 4244-4246.

Pokrop, R., Bajer, I.K., Wielgus, I., Zagorska, M., Albertini, D., Lefrant, S., Louarn, G. and Pron, A. (2009). Electrochemical and Raman spectroelectrochemical investigation of single-wall carbon nanotubes–polythiophene hybrid materials. *Synthetic Metals.* 159: 919-924.

Qin, S., Qin, D., Ford, W. T., Resasco, D. E. and Herrera, J. E. (2004). Functionalization of single-walled carbon nanotubes with polystyrene via grafting to and grafting from method. *Macromolecules.* 37: 752-757.

Rajarajeswari, M., Iyakutti, K. and Kawazoe, Y. (2012). Noncovalent and radicals covalent functionalization of a (5, 0) single-walled carbon nanotube with alanine and alanine. *Journal of Molecular Modeling*. 18: 771-781.

Rajiv, K., Jitendra, K., Amit, K., Vikram, K., Rama, K. and Ramadhar, S. (2010). Poly(3-hexylthiophene):Functionalized single-walled carbon nanotubes: (6,6)-phenyl-C61-butyric acidmethyl ester composites for photovoltaic cell at ambient condition. *Solar. Energy Materials. & Solar Cells*. 94: 2386-2394.

Rarvikar, N. R., Schadler, L. ., Vijaaraghavan, A., Zhao, Y., Wei, B. and Ajayan, P. M. (2005). Synthesis and characterization of thickness-aligned carbon nanotube-polymer composite films. *Chemical Materials*. 17: 974-983.

Razykov, T. M., Ferekides, C. S., Morel, D., Stefanakos, E., Ullal, H. S. and Upadhyaya, H. M. (2011). Solar photovoltaic electricity: Current status and future prospects. *Solar Energy.* 85: 1580-1608.

Saito, R, Fujita, M., Dresselhaus, G. and Dresselhaus, M. S. (1992). Electronic structure of chiral graphene tubules. *Applied physics letters.* 60: 2204-2206.

Sahoo, N. G., Chae, Y. Jung, So. H. H., Chob, J. W. (2007). Polypyrrole Coated Carbon Nanotubes: Synthesis, Characterization, and Enhanced Electrical Properties. S*ynthetic Metals.* 157: 374-379.

Salaneck, W. R., Friend, R. H. and Brédas, J. L. (1999). Electronic structure of conjugated polymers, consequence of electron-lattice coupling. *Physics Reports*. 319: 231-251.

Salvetat, J. P., Bonard, J. M., Thomson, N. H., Kulik, A. J., Forró. L., Benoit, W. and Zuppiroli, L. (1999). Mechanical properties of carbon nanotubes. *Apllied physics A: Materials science and processing*. 69: 255-260.

Sandler, J., Shaffer, M. S. P, Prasse, T., Bauhfer, W., Schulte, K. and Windle, H. (1999). Development of a dispersion Process for carbon nanotubes in an epoxy matrix and the resulting electrical properties. *Polymer.* 40: 5967-5971.

Savenije, T. J., Kroeze, J. E., Yang, X. and Loos, J. (2006). The formation of crystalline P3HT fibrils upon annealing of a PCBM:P3HT bulk hetero-junction. *Thin Solid Films*. 511512: 2-6.

Saxena, V. and Malhotra, B. D. (2003).Prospects of conducting polymers in molecular electronics. *CurrentApplied Physics.* 3: 293-305.

Scharber, and Sariciftci. (2013). Efficiency of bulk-heterojunction organic solar cells. *Progress in Polymer Science.* 38: 1929-1940.

Schôn, H. and Kloc, C. (2001). Organic Metal-semiconductor field effect phototransistor. *Applied Physics Letter*. 78: 3538-3540.

Schroder, E. and Hyldgaard,P. (2003). Van der Waals interactions of parallel and concentric nanotubes. *Materials Science and Engineering C. 23:721-725*

Scully, M., Petty, M. C. and Monkman, A. P. (1993). Optical properties of polyaniline thin films. *Synthetic Metals*. 55: 183-187.

Shaheen, S. E., Brabec, C. J., Sariciftci, N. S., Padinger, F., Fromherzet, T. and Hummelen, J. C. (2001). 2.5% efficient organic plastic solar cells . *Applied Physics. Letter.* 78: 841-843.

Shanmugharaj, A. M., Bae, J. H., Nayak, R. R. and Ryu, S. H. (2007). Preparation of poly(styrene-co- acrylonitrile) - grafted multiwalled carbon nanotubes via surface-initiated atom transfer radical polymerization. *Journal of Polymer Science Part A: Polymer Chemistry.* 45: 460-470.

Shim, M. and Siddons, G. P. (2003). Photoinduced conductivity changes in carbon nanotube transistors. *Applied physics letters*. 83: 3564-3566.

Stewart, D. A. and Léonard, F. (2005). Energy conversion efficiency in nanotube optoelectronics. *Nano letters*. 5: 219-222.

Strano, M. S., Dyke, C. A., Usrey, M. L., Barone, P. W., Allen, M. J., Shan, H., Kittrell, C., Hauge, R. H., Tour, J. M. and Smalley, R. E. (2003). Electronic Structure Control of Single-Walled Carbon Nanotube Functionalization. *Science.* 301: 1519-1522.

Tang, C. W. (1986). Two-layer organic photovoltaic cell . *Applied Phyics. Lett*er. 48: 183-185.

Tehrani, Z., Korochkina, T., Govindarajan, S., Thomas, D. J., Mahony, J. O., Kettle, J., Claypole, T. C. and Gethin, D. T. (2015). Ultra-thin flexible screen printed rechargeable polymer battery for wearable electronic applications. *Organic Electron*ics. 26: 386-394.

Thess, A., Lee, R., Nikolaev, P., Dai, H., Petit, P., Robert, J., Xu, C., Lee, Y. H., Kim, S. G., Rinzler, A. G., Colbert, D. T., Scuseria, G. E., Tománek, D., Fischer, J. E. and Smalley, R. E. (1996). Crystalline ropes of metallic carbon nanotubes. *Science.* 273: 483-487.

Tauc, J. (1974). Amorphous and Liquid Semiconductors, New York. *Plenum.*

Urbach, F. (1953). The Long-Wavelength Edge of Photographic Sensitivity and of the Electronic Absorption of Solids. *Physical review B*. 92: 1324-1324.

Veldman, A., Meskers, S. C. J. and Janssen, R. A. J. (2009). The energy of charge-transfer

states in electron donor–acceptor blends: insight into the energy losses in organic solar cells. *Advanced Functional Materials.* 19: 1939-1948.

Vijayakumar, C., Balan, B., Kim, M. J. and Takeuchi, M. (2011). Noncovalent Functionalization of SWNTs with Azobenzene-Containing Polymers: Solubility, Stability, and Enhancement of Photoresponsive Properties. *ACS Journal of Physical Chemistry C*. 115: 4533-4539.

Vignolo, P., Farchioni, R. and Grosso, G. (2001). Tight Binding Effective Hamiltonians for the Electronic States of Polyaniline Chains. *Physica Status Soldi*. 223: 853.

Viswanathan, G., Chakrapani, N., Yang, H., Wei, B., Chung, H., Cho, K., Chang, Y. R. and AjayanPulickel, M. (2003). Single-step in situ synthesis of polymer-grafted single-wall nanotube composites . *Journal of Americain Chemical Society*. 125: 9258-9259.

Wu, W., Li, F., Nie, C., Wu, J., Chen, W., Wu, C. and Guo, T. (2015).Improved performance of flexible white hybrid light emitting diodes by adjusting quantum dots distribution in polymer matrix. *Vacuum.* 111: 1- 4.

Wang, Y., Gao, L., Sun, J., Liu, Y., Zheng, S. and Kajiura, H. (2006). An integrated route for purification, cutting and dispersion of single-walled carbon nanotubes. *Chemical Physics Letters*. 432: 205-208.

Wang, Y., Zhang, S.and Deng, Y. (2016). Semiconductor to metallic behavior transition in multi-wall carbon nanotubes/ polyaniline composites with improved thermoelectric properties. *Materials Letters. 164*: 132-135.

Xue, M. A., Uchida, S., Rand, B. P. and Forrest, S. R. (2004). 4.2% efficient organic photovoltaic cells with low series resistances. *Applied Physics Letter.* 84: 3013-3015.

Yang, X., Loos, J., Veenstra, S. C., Verhees, W. J. H., Wienk, M. M., Kroon, J. M., Michels, M. A. J. and Janssen, R. A. J. (2005). Nanoscale Morphology of High-Performance Polymer Solar Cells. *Nano Letters*. 5: 579-583.

Yang, Z. P., Ci, L., Bur, J. A. N., Lin, S. Y., and Ajayan, P. M. (2008). Experimental observation of an extremely dark material made by a low-density nanotube array. *Nano letters*. 8: 446-451.

Yu, M. F., Files, B. S., Arepalli, S. and Ruoff, R. S. (2000). Tensile loading of ropes of single wall carbon nanotubes and their mechanical properties. *Physical Review letters*. 84: 5552-5555.

Yun, D., Feng, W., Wu, H., Li, B. , Liu, X., Yi, W., Qiang, J., Gao, S. and Yan. (2008). Controllable functionalization of single-wall carbon nanotubes by in situ polymerization method for organic photovoltaic device.*Synthetic Met*als. 158: 977-983.

Zaidi, B., Bouzayen, N., Wéry, J., Alimi, K. (2010). Grafting of oligo-N-vinyl carbazole on single walled carbon nanotubes, Journal of Molecular Structure. *Journal of Molecular Struct*ure. 971: 71-80.

Zaidi, B., Ayachi, S., Mabrouk, A., Molinie, P. and Alimi, K. (2003). Changes of the properties of poly-phenylene-vinylene-ether and C1_4 poly-phenylene-vinylene-ether with iodine pressure and annealing. *Polymer Degradation and Stability*. 79: 183-192

Zaidi, B., Bouzayen, N., Wéry, J. and Alimi, K. (2011). Annealing treatment and carbon nanotubes concentration effects on the optical and vibrational properties of single walled carbon nanotubes functionalized with short oligo-N-vinyl

carbazole.*Materials Chemistry and Physics.* 126: 417-423.

Zaidi, B., Bouzayen, N., Znaidia, S. and Mbarek, M. (2013). Changes of the properties of poly-phenylene-vinylene-ether and C1-4 poly-phenylene-vinylene-ether with iodine pressure and annealing. *Journal of Molecular Structure*. 1039: 46-50.

Zhang, L. and Wan, M. (2003). Self-Assembly of Polyaniline—From Nanotubes to Hollow Microspheres.*Advanced Functional Materials.* 13: 815-820.

Zhang, J., Zou, H., Qing, Q., Yang, Y., Li, Q. and Liu, Z. (2003). Effect of Chemical Oxidation on the Structure of Single-Walled Carbon Nanotubes. *The Journal of Physical Chemistry* B. 107: 3712-3718.

Zhang. Y. and Iijima. S. (1999). Elastic reponse of carbon nanotube bundles to visible light. *Physical Review Letter*. 82: 3472-3475.

Zheng, M., Jagota, A., Strano, M. S., Santos, A. P., Barone, P., Chou, S. G., Diner, B. A., Dresselhaus, M. S., Mclean, R. S., Onoa, G. B., Samsonidze, G. G., Semke, E. D., Usrey, M. and Walls, D. J. (2003). Structure-Based Carbon Nanotube Sorting by Sequence-Dependent DNAAssembly. *Science.* 302: 1545-1548.

Zhokhavets, U., Erb, T., Hoppe, H., Gobsch, G. and Sariciftci, N. S. (2006). Effect of annealing of poly(3-hexylthiophene)/fullerene bulk heterojunction composites on structural and optical properties. *Thin Solid Films.* 496: 679-682.

Zhou, Y., Freitag, M., Hone, J., Staii, C., Johnson, A.T. J., Pinto, N. J. and MacDiarmid, A. G. (2003). Fabrication and electrical Characterization of polyaniline based nanofibers with diameyter below 30 nm. *Applied Physics Letter.* 83: 3800-3802.

Zhou, X., Ren, A. M. and Feng, J. K. (2004). Theoretical investigation on the ground- and excited-state properties of novel octupolar oligothiophene-functionalized truxenes and dipolar analogs. *Polymer.* 45: 7747-7757.

Zhu, H., Wei, J., Wang, K. and Wu, D. (2009). Applications of carbon materials in photovoltaic solar cells. *Solar Energy Materials and Solar Cells*. 93: 1461-1470.

Zou, L. Y., Ren, A. M., Feng, J. K., Ran, X. Q., Liu, Y. L. and Sun, C. C. (2009). Structural, electronic, and optical properties of phenol-pyridyl boron complexes for light emitting diodes. *International Journal of Quantum Chemistry.* 109: 1419-1429.